INTEGRATED GEOPHYSICAL INVESTIGATIONS OF METALLIC MINERALS IN PRE-CAMBRIAN SHIELD ROCKS OF WAD SAYYIDAN AREA CHINIOT PUNJAB (TOPOSHEET NO.44-A/13)

MUHAMMAD KAMRAN
MPhil (GEOPHYSICS)
2021-2023

DEPARTMENT OF EARTH SCIENCE
QUAID-I-AZAM UNIVERSTY ISLAMABAD
PAKISTAN

INTEGRATED GEOPHYSICAL INVESTIGATIONS OF METALLIC MINERALS IN PRE-CAMBRIAN SHIELD ROCKS OF WAD SAYYIDAN AREA CHINIOT PUNJAB (TOPOSHEET NO.44-A/13)

BY

MUHAMMAD KAMRAN
MPhil (GEOPHYSICS)

SUPERVISED BY

DR. AAMIR ALI

DEPARTMENT OF EARTH SCIENCE
QUAID-I-AZAM UNIVERSTY ISLAMABAD
PAKISTAN

“In the Name of ALLAH, the Most Merciful & Mighty”

“PAY THANKS TO ALLAH EVERY MOMENT AND GO TO EXPLORE THE HIDDEN TREASURES, ITS ALL FOR YOUR BENEFIT”

(AL-QURAN)

CONTENTS

Topics **Chapter** **Page**

List of Figures

List of Tables

CERTIFICATE

This dissertation submitted by **Mr. MUHAMMAD KAMRAN S/O MUHAMMAD RAFIQ CHUGHTAI** is accepted in its present form by the Department of Earth Sciences, Quaid-I-Azam University Islamabad as satisfying the requirement for the award of MPhil degree in Geophysics.

RECOMMENDED BY

DR. AAMIR ALI _____

Supervisor &
Chairman of Department

EXTERNAL EXAMINER _____

DEPARTMENT OF EARTH SCIENCES
QUAID-I-AZAM UNIVERSITY
ISLAMABAD
2021-2023

DEDICATION

“This dissertation is dedicated to ALLAH, the almighty”
“His prophet HAZRAT MUHAMMAD (P.B.U.H)”.

&

To My Parents, Family and Respected Teachers as without your prayers, support and your trust in me it was not possible for me to achieve this kind of success. May Allah always keep your shadow upon me andshower His blessing upon you.

&

To My Department of Earth Sciences, (QAU)
and
Geological Survey of Pakistan (GSP)

ACKNOWLEDGEMENT

In the name of Allah, the most Beneficent and the most Merciful. All praises to Almighty Allah, the Creator of universe, who blessed me with the health and knowledge. I bear witness that Holly Prophet Muhammad (PBUH) is the last messenger, whose life is a perfect model for the whole mankind till the Day of Judgment. Allah blessed me with knowledge related to the earth. I am enabled by Allah to complete my work. Without the blessings of Allah, I would not be able to complete my work and to be at such a place.

I am indebted to my honorable supervisor **Dr. Aamir Ali (HOD)** for giving me an initiative to this study. There inspiring guidance, dynamic supervision and constructive criticism, helped me to complete this work in time. I pay my thanks to the whole faculty of my department, whose assistance and cooperation build my moral during my studies.

I am very thankful to Senior management of **Geological Survey of Pakistan (GSP)** and **Mines and Minerals Department Punjab (MMDP)** for their help and support especially the respected **Mr. Muhammad Saeed, Chief Geophysicist** from **GSP** whose valuable knowledge, assistance, cooperation and guidance enabled me to take initiative, develop and furnish my academic carrier.

I am also thankful to all my class fellows for their moral support and respect given to me during the MPhil. They helped me a lot and I am unable to forget their efforts. I pay my thanks to the employees of clerical office who helped me a lot and all those their names do not appear here who have contributed to the successful completion of this study.

I specially acknowledge my **Parents** and **Family**, for their encouragement, endless love, support and sacrifices throughout the study.

MUHAMMAD KAMRAN
M.Phil. (Geophysics)
2021-2023

ABSTRACT

Pre-Cambrian Shield Rocks have always been attractive target for valuable metallic minerals exploration all over the world. In Pakistan these rocks are exposed in Sargodha, Shah Kot, Sangla Hill (Punjab), and Nagar Parker area of Sindh Province. Geological Survey of Pakistan and Mines and Mineral Department, Government of Punjab, initiated a joint venture project in 2013 for the exploration of metallic minerals.

The project includes the coverage of 28 toposheets by semi-detailed magnetic survey and followed by three promising zones with detailed integrated geophysical surveys. Gravity, magnetic and IP/Resistivity surveys were included in the detailed integrated survey. In 28 toposheets the areas of Sargodha, Faisalabad, Chiniot, Hafizabad, Shahkot, Sangla hill, Nankana Sahib, Sheikhupura, Lahore, Kot Radha Kishan, some part of Changa Manga Forest etc. are included by covering an area of about 18000 Square kilometers.

The Topo Sheets included are 44-A/9, **44-A/13**, 44-A/14, 44-A/15, 43-D/12, 43-D/16, 44-E/1, 44-E/2, 44-E/3, 44-E/6, 44-E/7, 43-H/4, 43-H/8, 43-H/12, 43-H/16, 44-E/5, 44-E/9, 44-E/13, 44-I/1, 44-E/10, 44-E/11, 44-E/12, 44-E/14, 44-E/15, 44-E/16, 44-I/2, 44-I/3 & 44-I/4. The data acquisition started in August, 2013 and continued till December, 2015. The Semi-detailed magnetic stations were observed along all the mattled and un-mattled accessible tracks present in the area at approximately 500 meters interval. The semi-detailed magnetic map of the area shows two parallel NW-SE trending faults. The majority of the demarcated 32 magnetic anomalies lie on the same inferred faults.

Based on the semi-detailed magnetic survey, three areas **Wad Sayyidan**, Ghutti Sayyidan and Chak Jhumra were selected for detailed integrated geophysical survey. The areas are in close proximity of already discovered Chiniot and Rajoa Iron ores. A grid spacing of 50 x 50 meters in Wad Sayyidan was laid. About 9600 gravity and same number of magnetic stations were observed in Wad Sayyidan area. Similarly, 55 IP/Resistivity points were observed down to the depth of 1000 meters in Wad Sayyidan area, respectively.

The gravity signature of the anomalies is also supporting the presence of concealed subsurface fault in the areas of investigation and magnetically susceptible

material has most probably been emplaced along the fractured weak zone. In general, in Punjab plains, bouguer gravity effects are closely correlated with the subsurface topography of basement rocks. However, the magnetic signature in shallow basement rocks as inferred from Vertical Electrical Soundings with high gravity show the presence of magnetically susceptible minerals like magnetite.

The IP signal in Wad Sayyidan area has quite a large variable range as compared to the other two areas (Ghutti Sayyidan & Chak Jhumra) where the detailed studies were carried out. The large values of chargeability are observed at the edges of the positive gravity closures. These large values of chargeability normally correspond to the sulphide mineralization like copper, gold, zinc, lead etc.

Test drilling is recommended based on the results of the integrated geophysical surveys for the confirmation of subsurface picture of geology and the causative source generating the anomalous gravity, magnetic, and IP effect.

CHAPTER NO. 1

INTRODUCTION

1.1 Introduction

Pre-Cambrian Shield rocks are considered to host valuable metallic minerals. In Pakistan, these rocks are exposed in Sargodha, Chiniot, Sangla Hill and Nagar Parker. OGDCL carried out an aero-magnetic survey over a part of Punjab and prepared a Total Field Magnetic Intensity Anomaly Map. A small, high amplitude magnetic anomaly was depicted near Chiniot.

Geological survey of Pakistan detected a sharp magnetic anomaly during 1985 by carrying out magnetic survey. Three drill holes were drilled by GSP after carrying out detailed integrated geophysical survey over the anomaly to ascertain the presence of mineralization. Two drill holes showed the presence of high-grade iron along with showings of other precious minerals like copper and gold.

Geological Survey of Pakistan and Mines & Mineral Department, Government of Punjab, initiated a joint venture project in 2013. Initially, 28 toposheets, covering an area of about 18000 Square Kilometer by Semi-detailed Magnetic Survey. The semi-detailed magnetic survey demarcated about 32 anomalous zones which were recommended for further work.

Three anomalies out of 32 namely, Wad Sayyidan, Ghutti Sayyidan and Chak Jhumra areas were selected initially for Integrated Geophysical Survey (Gravity, Magnetic and Induced Polarization (IP)/Resistivity) due to the proximity of already discovered Chiniot Iron Ore.

The study area is Wad Sayyidan which is one of the anomalous zones out of the above mentioned three anomalies selected for detailed surveys. The semi-detailed and detailed data acquisition surveys are done in two phases. The details of the surveys conducted in Wad Sayyidan area are discussed in the Table 1.1.

Table. 1.1: Details of Wad Sayyidan area covered during study.

S.NO.	PHASES	DURATION	SURVEY	TOPO SHEETS/AREA
1	Phase-I	Aug-Oct, 2013	Semi-detailed magnetic	44A/13/ Wad Sayyidan
2	Phase-II	May 2014 – Dec. 2015	Detailed Gravity, Magnetic, IP/Resistivity	44A/13/ Wad Sayyidan

1.2 Location and Accessibility

The major cities near the study area included are Chiniot, Sargodha, Faisalabad. Rock exposures are present near Sargodha, Chiniot and Sangla Hill areas. Very good condition metaled roads and Railway Tracks connects the whole area with the other parts of the country. Lahore-Faisalabad motorway also passes through the area under investigations. The area is bounded by 31º 0′ N to 32 º 15′ N and 72 º 30′ E to 74 º 15′ E (Fig.1.1, Fig.1.2, and Fig.1.3).

1.3 Period of Investigations

The semi-detailed investigations started in August 2013 and were completed in November 2015. The detailed geophysical investigations were started in May 2014 and completed in December 2015.

1.4 Previous Work

OGDCL conducted an aeromagnetic survey over Potohar Platue and a part of Punjab Plains with the help of technical experts from former USSR. A positive magnetic anomaly was detected with 635 Gammas amplitude south of Chiniot. Geological Survey of Pakistan conducted detailed integrated geophysical survey (Gravity, Magnetic, Resistivity and Seismic) in the period of 1982 to 1989. Three drill holes were drilled and two of them showed high grade iron ore along with the presence of precious minerals like copper and gold (Butt et al, 1993).

1.5 Climate and Weather Conditions

Severe weather conditions prevail in the area with temperatures in high forties in summer and humid in July to September and down to 0 ˚C in winters. Fog also covers

the big area of Punjab including Chiniot and surrounding areas. The area remains foggy in December to January.

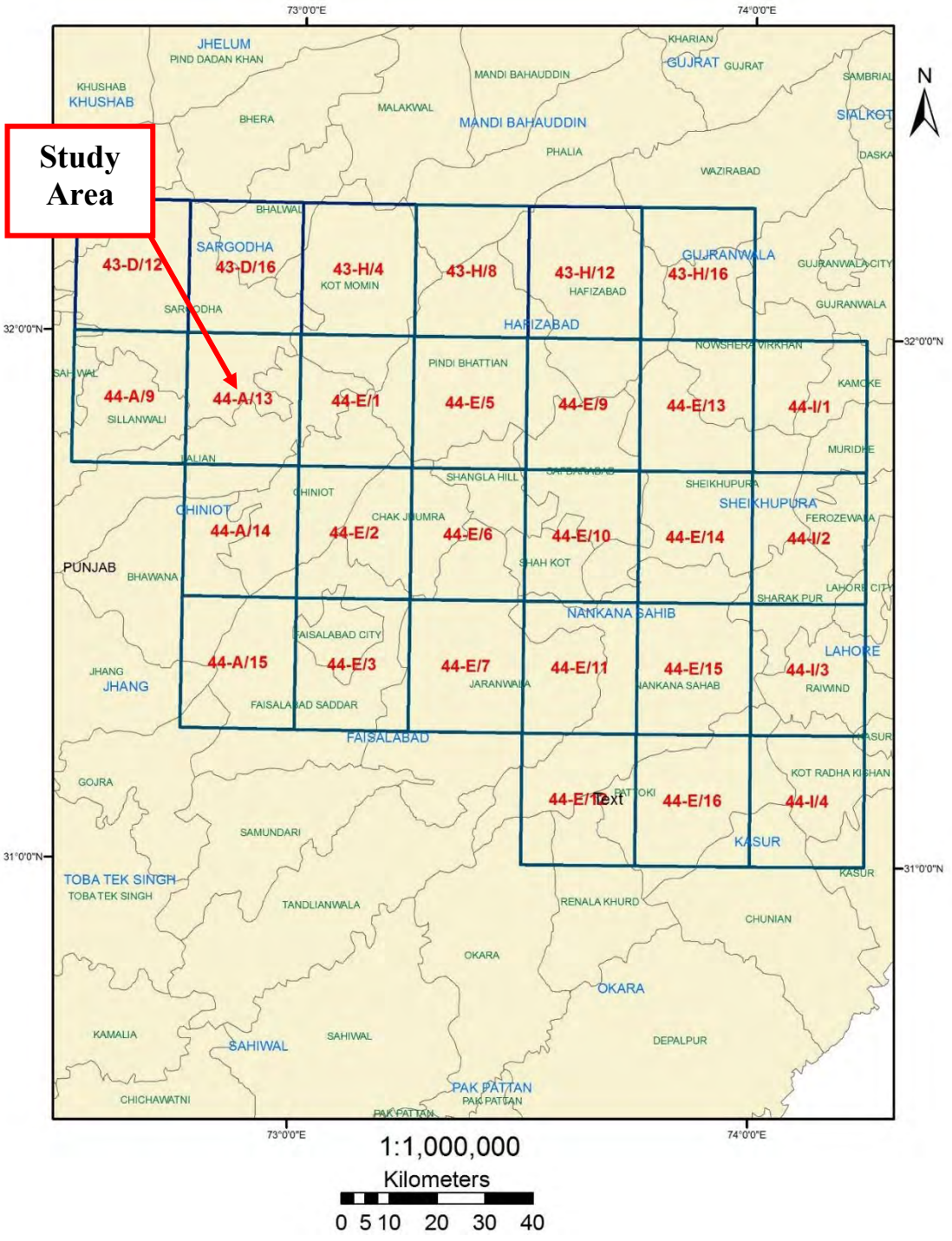

Fig. 1.1: A map depicting the different toposheets of Punjab, Pakistan. The study area Wad Sayyidan has been marked on the toposheet no. 44-A/13.

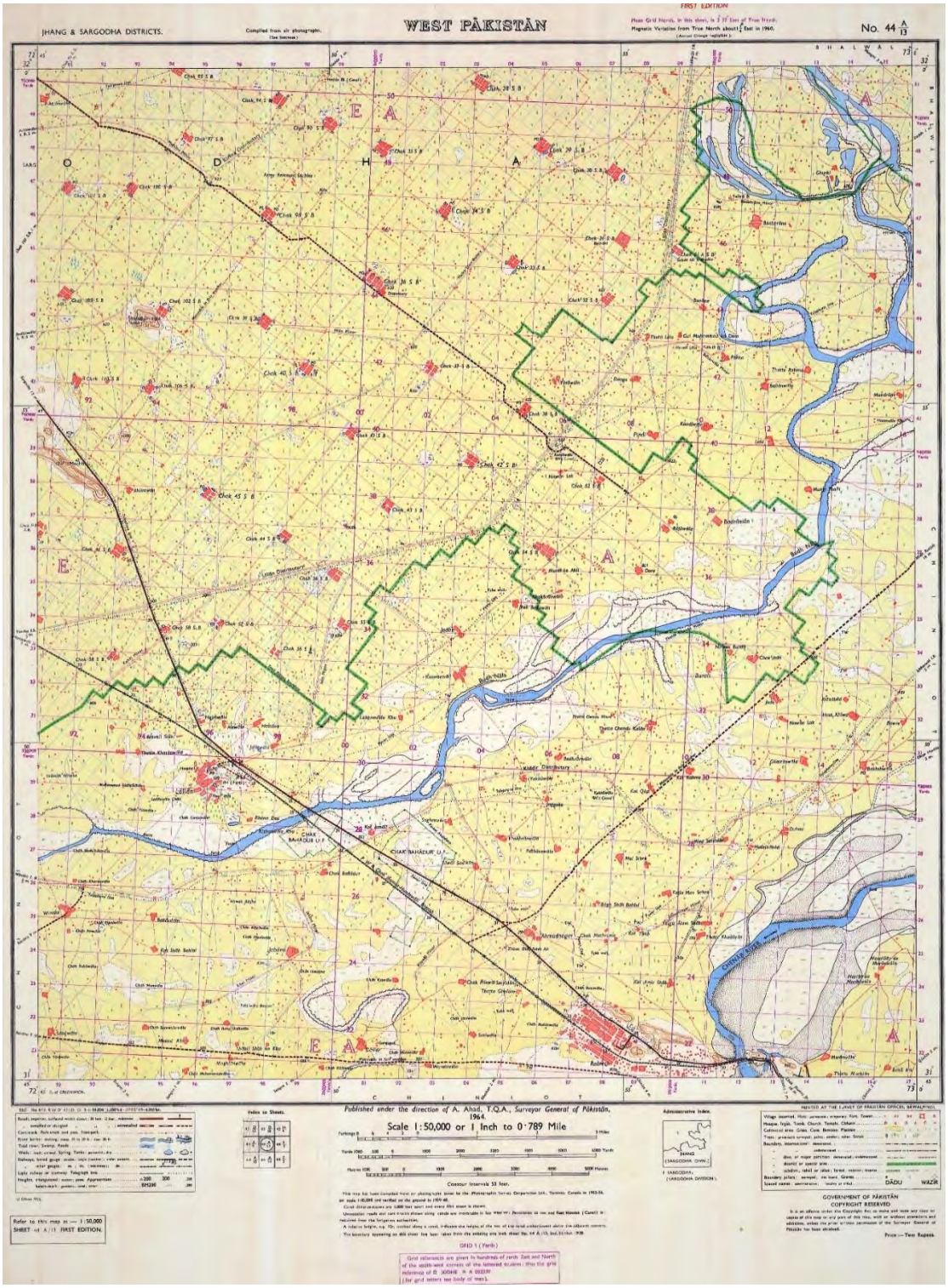

Fig. 1.2: The toposheet no. 44-A/13 which covers the study area Wad Sayyidan, District Chiniot, Punjab, Pakistan.

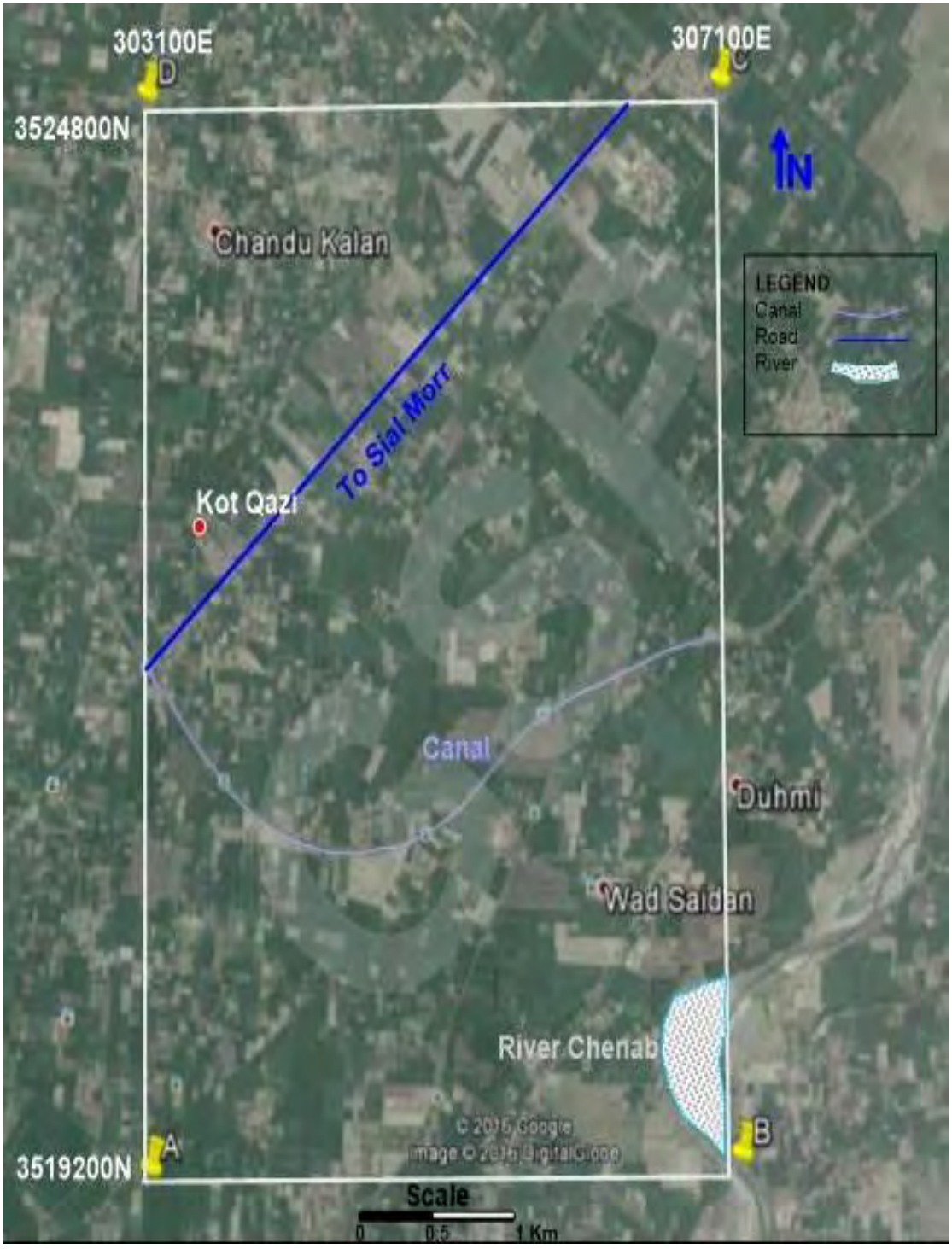

Fig. 1.3: Location map (Google map) of the study area, Wad Sayyidan, District Chiniot, Punjab, Pakistan.

CHAPTER NO. 2

GEOLOGY, TECTONICS & STRATIGRAPHY

2.1 Introduction

Kirana Hills are the remnants of extensive igneous activity occurred during Precambrian within Kirana-Malani Basin of NE Gondwana and represents an isolated outcrop scattered in the Punjab Plain from Chiniot to Sargodha (Chaudhary et al., 1999; Shah, 1977). The Volcanics of Kirana Hills are mainly comprised of mafic and felsic rocks however, the Atomic Energy Minerals Centre Lahore, mineralogy division also confirmed the presence of intermediate rocks in complex. These rocks belong to the tholeiitic basalt-rhyolite magma association with intercalated meta-sediments.

Tectonically, the area lies on the bulge of the Indian plate which was formed after the Indian plate collides Eurasian plate. Kirana hill represent the western extension of the Precambrian shield of India (Kazmi and jan,1997). This NW -SE trending Sargodha-Shah Kot ridge, which is parallel to major structures in the central Himalayas (Powell, 1979) is an extension of the Aravalli Mountain belt of Rajhistan, where it is characterized by a NE-SW trend, conspicuously displayed from Champnar in Gujarat at the head of the Gulf of Cambay to near Delhi, across Rajhistan. Near northern end of the Aravalli range around Delhi, a part of the structure turns sharply towards the northwest and NNW and continues as subsurface ridge bordering the Punjab plains and extends to Kirana and Sangla Hills not far from the eastern end of the Salt Range.

This ridge is believed to be the flexure bulge of the Indian plate, which is seismically active. This zone coincides with a continuous zone of seismicity (recorded by the Tarbella network), which strikes parallel to Himalayas but is 200 Kms south of the main boundary thrust (Seeber and Armbuster, 1977). The surface exposure of this zone is the Sargodha – Shahkot buried ridge. The zone typically experiences low magnitude seismicity, and this seismicity is believed to be due to the release of tension accumulated on the flexure bulge of the Indian plate from time to time, although the rate of tectonic strain release is very low in the area (Kazmi and Jan, 1997).

The igneous suite dated age on basis of Rb-Sr is 870±40 Ma (Davis and Crawford 1971). Precambrian basement rocks in the alluvial plains of the Punjab ranging from 100 m^2 to 20 Km^2 in the SE of Sargodha (Kazmi and Jan, 1997).

2.2 Location and Accessibility

The study area lies 10 Km south of Sargodha city and is located in the Kirana Hills (Lat 31°, 51", 30" to 31°, 59', 30" Long, 72°, 39', 30 TO 72°, 46", 57"). The railway track within this region connects different hills namely, Blund, Sheikh, Hachi, and Hundewale. The Precambrian rocks are exposed in a few isolated hills near Kirana, Chiniot, Shahkot, and Sangla in the Punjab Plains. The area of Wada Sayyidan, Ghutti Sayyidan and Chak Jhumra and Chak Jhumra are located in surroundings of Chiniot Hills outcrops.

2.3 Physiography

The topographic features of Kirana Hills are unusual, as they are in the form of isolated hills scattered in the flat. Plain which as give an impression of a buried mountain. Generally, the color of the rocks is dark brown, and they are without any vegetation, General trend of the strata is northwest-southeast. The relief of the Kirana hills is 240 meters, and altitude varies from 268 meters to 508 meters above seas level. The highest point is located at Kirana Hill. (500 meters).

No stream of any significance originates from the area. The hills are not capped by any alluvium or soil, so they are without any vegetation.

2.4 Previous Work

Kirana hills are the best example of bimodal continental magmatism. Following workers studied a reconnaissance map on 1:63,360 scale presented by Heron (1913) in which they studied the Precambrian rock of the area. Ibrahim Shah of GSP carried out reconnaissance of the area and reported the presence of gold in Kirana Hill (Shah 1973). Alam at el (1972) prepared a geological map of the area on 1:10,000 scale. (Alam and other 1972). In 1987, Alam subdivided the Kirana Group on the basis of mapping

carried out earlier, and published report on geology of Kirana Hills (Alam 1987). Khan et al., (2009) carried out research on petrography and mineralogy of dolerites of Hachi Volcanics in Kirana Hills. Khan et al., (2027) conducted Petrographic and Geochemical Analyses of Kirana Hills Shield Rocks near Sargodha area.

2.5 Geology and Stratigraphy of the Area

Kirana hill are basically composed of metasediments and volcanic and are divided into older Kirana group and younger Sharaban Group (Alam, 1987). Kirana group comprises of three formations Asianwala, Taguwali and Hachi volcanic. Chaudhary et al., (1999) Further modified the stratigraphy of the Kirana Hills and introduced two main Groups, Hachi Volcanics and Machh Super Group (Table-). Hachi Volcanics Group is further categorized into two formations,

Volcanics and Volcanogenic Slates, which are mainly comprised of andesites, dacites, dacitic tuff, dolerites, rhyolitic tuff, and rhyolites. Machh Super Group contains five formations which include Chak 112 Conglomerates, Taguwali Formation, Asianwala Formation, Hadda Formation, and Sharaban Formation (Table-). The major lithologies of these formations are conglomerate, Slates, fine grained quartz wackes / arenaceous slates, Phyllite and Quartzite. The rocks exposed in the study area are categorized into Meta-sedimentary and Igneous rocks.

2.6 Meta-Sedimentary Rocks

These rocks are present in the study area are slates, quartzite, and phyilites, and have igneous acidic and basic rock intrusions. The detailed description of each rock type is given below:

2.6.1 Quartzites

The major composition of the quartzites is quartz (about 95 %) with traces of clay minerals such as sericite (Adams et al., 2017). Quartzites have a granular and coarse texture with the presence of arenites (ZhgarikovF, 2007). The quartzites of the Kirana Hill are courser relative to the finer quartzites of the Hill Chak No. 111 (Malkani

and Mahmood, 2016). Some variation of fine-grained quartzites with interbedded slates and clay minerals (about 10 %) are present (ZhgarikovF, 2007).

2.6.2 Slates

Slates are metamorphosed shales with the mineral variation of 70 to 80 % clay and 20 to 30 % other mineral. The color of slates varies from medium to dark grey. The slates of the Panjab plains are mainly exposed in Chander and Tagu-Wali Hills and are interbedded with fine-grained quartzites and phyilites (Khan et al., 2009).

2.6.3 Phyllites

Phyllites are fine grained, light grey colored thin beds comprising of 40 to 50 % quartz and 25 to 30 % clay (Naeem et al., 2019). Within the Kirana Hill, phyllites are exposed towards south and their outcrop is also found in the Taguwali and Moch Hills (Haider et al., 2021).

2.7 Igneous Rocks

2.7.1 Volcanic Breccia and Tuffs

The volcanic breccia and tuffs have experienced slight metamorphism without losing their original texture and have inter-layering of slates and quartzites. The tuffs are mineralogically composed of 65 to 85 % groundmass (quarzitic microlites, glass, fine grained quartz, and feldspar) 15 to 35 % phenocrysts (perthitic feldspar, quartz, and rock fragments) (Davies and Crawford, 1971).

2.7.2 Lava Flows

Lava flows have interlayering meta-sediments making it difficult to distinguish from country rock. Different rocks such as decite, rhyolite, and andesite represent lava flows. The lava flows of Shaikh, Hachi, Buland, and Taguwali are mainly composed of medium to reddish grey rhyolite with a glassy matrix due to the presence of phenocrysts and mineralities. The dark grey, holocrystalline andesitic lava flows are found in

Shaheen Abad Hill comprising of 40 to 45 % orthoclase, 45 to 50 % plagioclase, and 5 to 7 % Hornblende along with its chlorite alteration (Chaudhry et al., 2022).

2.7.3 Basic Intrusive Bodies

The area also contains 300 m thick sheet-like sill bodies extended over hundreds of meters, intruding the country rocks along with the meta-sediments (Davies and Crawford, 1971). These dark greenish to grey, coarse grained, highly altered rocks are comprised of 15 to 33 % chlorite, 40 to 60 % plagioclase, 3 to 10 % quartz, 1 to 5 % ilmenite, and 1 to 15 % carbonate. These bodies are mainly exposed in Shaikh and Hachi Hill near Chak No. 123 SB (Davies and Crawford, 1971).

The basement rocks are exposed in Sargodha, Sangla, and Shahkot Hills (Gee and Gee, 1989). The Formations of Kirana Group dominantly contains grey slates, grey and red quartzite, and conglomerates. Some intrusion of the basic rocks in these formations are reported to be highly weathered and altered with the andesite containing hematite in veins along fractures. Stratigraphic units of Kirana Hills shown in Table.2.1 (Chaudhry et al., 2022).

Table. 2.1: Table showing the stratigraphic units of Kirana Hills (Chaudhry et al.,1999).

Group	Formation	Description
Machh Super Group	Sharaban Formation	Conglomerates with slate intercalations
	Hadda Formation	Calcareous quartiztes
	Asianwala Formation	Mainly quartzites with subordinate quartz wackes/arenaceous slates, gritty quartzites and slates, often showing cross bedding and ripple marks
	Tuguwali Formation	Slates, fine grained quartz wackes/arenaceous slates
	Chak 112 Conglomerates	Polymictic conglomerate with clasts of dolerite and acid volcanics
Hachi Volcanics	Volcanogenic slates	Often interbedded with rhyolite/ rhyolitic tuff and dolerite
	Volcanics	Dolerites, andesites, dacites, dacitic tuff, rhyolites and rhyolitic tuff

CHAPTER NO. 3

DATA ACQUSITION
(Magnetic, Gravity & Resistivity/IP)

3.1 Methodology

3.1.1 Identification of Case Study

Before performing any geophysical survey technique, it requires an objective or case study on which to perform geophysical investigation to solve that case. OGDCL carried out an aero-magnetic survey over the part of Punjab and prepared a Total Field Magnetic Intensity Anomaly Map. A small, high amplitude magnetic anomaly was depicted near Chiniot. Geological survey of Pakistan detected a sharp magnetic anomaly during 1985 by carrying out magnetic survey. Three drill holes were drilled by GSP after carrying out detailed integrated geophysical survey over the anomaly to ascertain the presence of mineralization. Two drill holes showed the presence of high-grade iron along with showings of other precious minerals like copper and gold.

So, based on above mentioned previous discoveries our main objective is to demark high magnetic anomalous zones by semi detailed magnetic survey and then perform detailed and integrated geophysical surveys (Like Magnetic, Gravity, Resistivity & IP) to confirm exact minerals, their location and ultimately propose drill holes for mineral exploration.

3.1.2 Geophysical Technique

As the case has been identified now, firstly the semi-detailed Magnetic Survey of the study area was performed. Then two passive geophysical techniques were selected. Detailed Gravity and Detailed Magnetic techniques were applied to investigate more about the study area, as Gravity will give us density variation while Magnetic will give us susceptibility variation in subsurface (Hinze et al., 2013). Finally, we use Resistivity & IP surveying geophysical technique for confirmation of proposed minerals and their depth for further exploration (Adel et al., 2022).

3.1.3 Purpose of Gravity, Magnetic and Resistivity/IP Survey

Gravity and magnetic surveys are conducted for prospecting of geology, and are also made for following purpose:

- To demarcate the areas in terms of tectonic, lithologic and petrographic units, which will be mainly used for geological mapping.
- To determine the size of deposit, elements of deposition and shape of structure enclosingthe whole deposition.
- To delineate the promising zones and areas for more detailed geological and geophysical exploration.
- For prospecting of mineral deposits accumulated in structure.
- To find the thickness of promising layer, depth of this layer and also to trace deep layingfaults.

Generally, gravity technique when integrated with magnetic technique can achieve the following purposes:

- The tectonic, lithologic and petrographic demarcation of areas for surface and subsurface geological mapping.
- The delineation of promising zones and areas for more detailed geological and geophysical exploration.
- The discovery of local structures favoring the location of minerals and thus indicating themineral deposits.
- The determination of the form, elements of deposits and size of deposits and of the structure enclosing and disclosing it.
- The data of gravity survey can also be employed to solve the geodetic problems.
- To study the depths of earth's crust, in order to evaluate its thickness, delineate it in separateblocks, and trace deep laying faults.

Gravity technique integrated with magnetic technique and finally with Resistivity/IP technique can achieve the following purposes:

- To estimate the resistivity and thickness of various subsurface strata for mineral and groundwater analysis.
- It detects the lateral and vertical variation of resistivity based on electrical response of subsurface layers.
- 3-dimensional anomalous structures can be delineated from the electrical conductivities.
- The IP is used for ore detection based on the variation of chargeability in the subsurface.

3.2 Planning of the survey

Preliminary planning was necessary for any geophysical work in order to facilitate the field operations and to solve other problems during the survey. The main objective of the planning was not only to save time and money but also to improve the quality of data and to get the maximum possible information. consideration in sequence of surveying pattern, data collection, data processing procedure provides an opportunity to enhance signal to noise ratio of data which is ultimately required in final interpretation of any geophysical survey.

3.3 Survey Design

For geophysical investigation of Wad Sayyidan area, the survey was designed in Google Earth pro.Survey designing demands the consideration of problem in hand as it critically affects both the geophysical technique, which is being used and the type of survey, for example ground survey, airborne survey or down hole. Survey design for geological mapping should have a uniform coverageof geophysical data across the area of interest. In ground gravity and magnetic survey, grid or profiling pattern are used depending upon the nature of the case study and location.

Considering the nature of the case, first in semi detailed magnetic survey data was observed at approximately 500 meters and in detailed magnetic and gravity survey the magnetic observations were taken along with the gravity observations on grid pattern. In Wad Sayyidan, a grid of 50 X 50 meters was established. The station

interval in a profile was set at 50 meters and the interval between the profiles is also 50 meters. In total, about 9600 stations were established on which the gravity and magnetic readings were measured. In Resistivity/IP survey, the technique which has been used is Vertical Electrical Sounding (VES) and a total of 55 VES surveys with the depth of investigation of 1 Km have been performed in the study area.

3.4 Magnetic Method

The earth has a bipolar magnetic field being generated in its outer core due to convection currents (Parker, 1970). The alignment of two poles of this magnetic field roughly in the north-south direction. This field induces magnetization in the rock bodies present at shallow depth (Gay, 1963). Magnetic anomalies depend on the shape, dimensions, depth and susceptibility of the subsurface bodies.

The magnetic data is used for the subsurface geological investigation based on the anomalous susceptibility response of the varying subsurface rocks (Abraham and Alile, 2019). Typically, the susceptibility of the underlying rocks is extremely variable due to the anisotropic nature of the earth. The bodies of interest detected by magnetic method include faults, dykes, and lava flows. The local magnetic field is proportional to the susceptibility of the rocks suggesting that the magnetically anomalous bodies will have a relatively strong magnetic field strength (Parasnis, 2012).

3.4.1 Data Acquisition in Semi-Detailed Survey

Ground data acquisition was performed with the help of Proton Precision Magnetometers (Geometrics 856-AX). Data was observed at approximately 500 meters spacing along all mattled, fair-weather motor-able tracks, paths along canals, distributaries, minors, along Nalas, Drains and even on foot when it deemed necessary. About 1050 magnetic stations were observed during semi detailed magnetic survey.

Due to the presence of High voltage power line crossing or intense man-made electromagnetic sources (as buildings, power lines, pipelines, telephone cables, electric and phone poles etc.) can distort the data, to avoid any noise, magnetic readings a safe distance was kept during the time of survey.

Data could not be observed in the close vicinity and inside of highly populated cities, inside villages, near industrial areas (due to presence of heavy machinery). The location of observed points was determined by handheld GPS (Garmin) in UTM coordinates system. The semi-detailed data acquisition observation points are shown in fig.3.1.

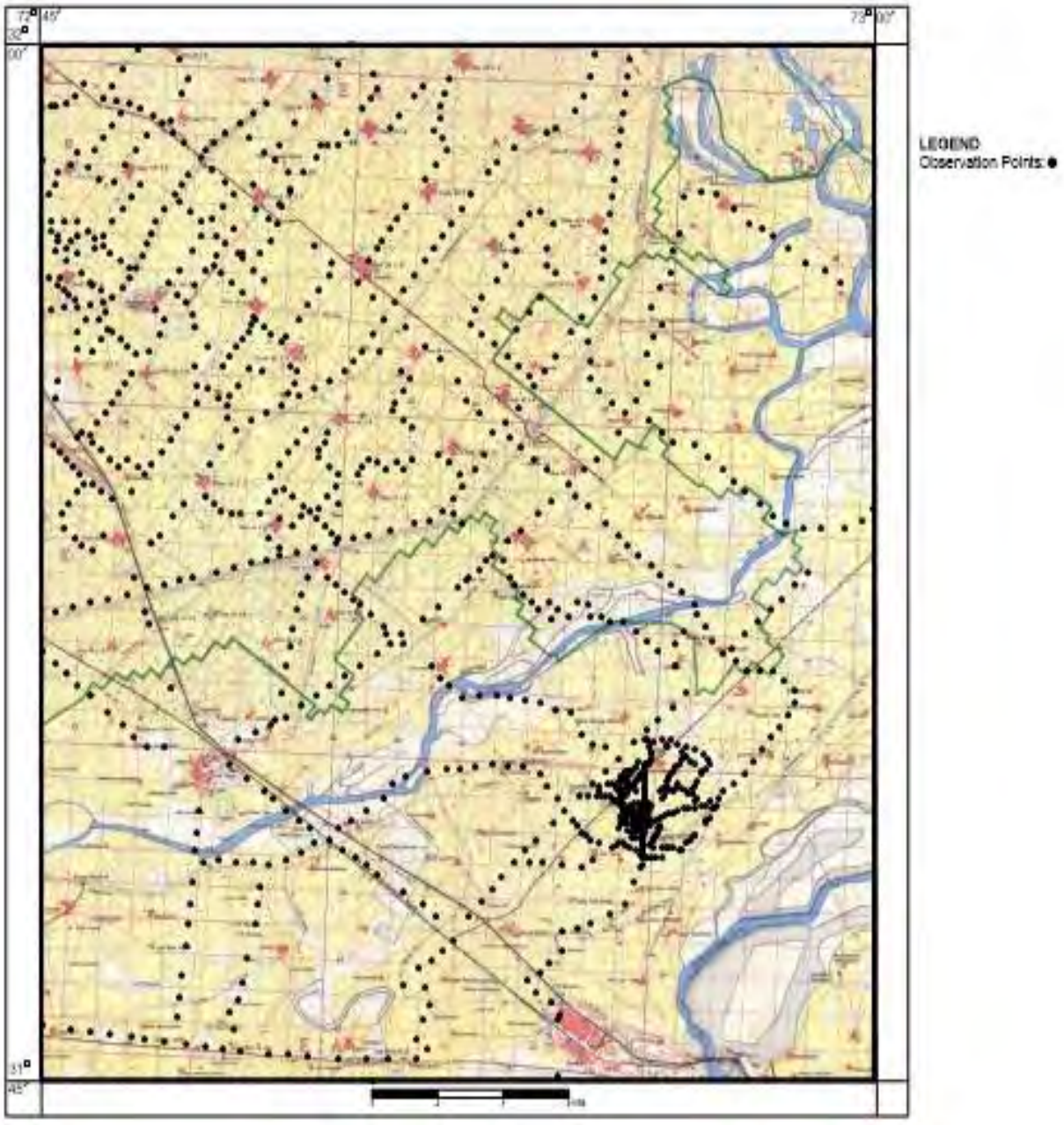

Fig. 3.1: Semi Detailed Magnetic Data Acquisition Observation Points of study area toposheet no.44-A/13 Wad Sayyidan.

3.4.2 Data Acquisition in Detailed Survey

The magnetic survey was carried out by using seven proton precession magnetometers at different time (Magnetometer, model No: G-856-AX, serial No.278807, 277675, 278150, 278151, 278152, 50068, 50069 of EG & G Geometric). Based on the semi-detailed magnetic survey, Wad Sayyidan (Study area), was selected for detailed integrated geophysical survey. The detailed data acquisition observation points are shown in fig.3.2.

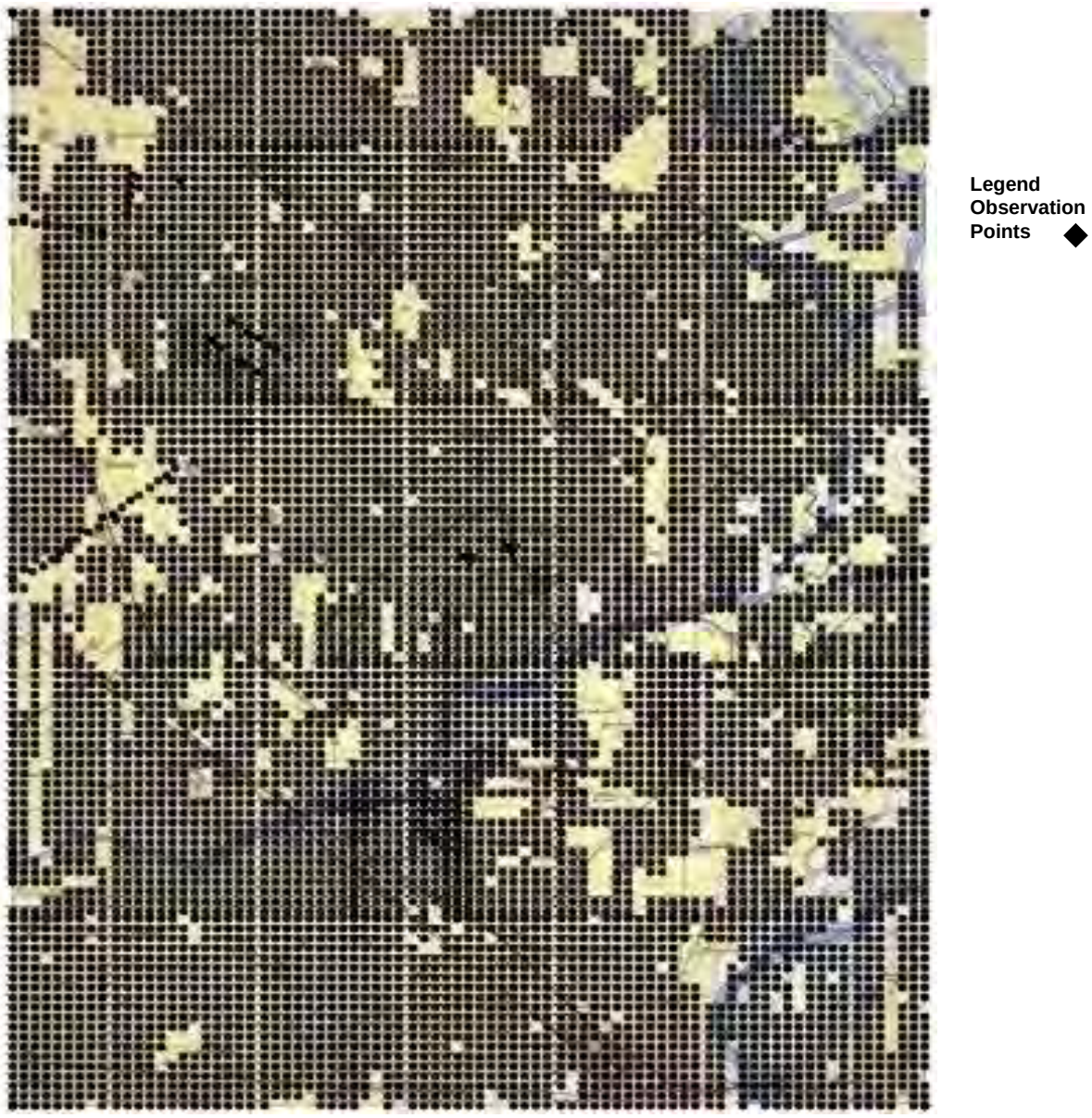

Fig. 3.2: Detailed Magnetic & Gravity Data acquisition observation points of study area toposheet no.44-A/13 Wad Sayyidan.

The areas are in close proximity of already discovered Chiniot and Rajoa Iron ores. A grid spacing of 50 x 50 meters in Wad Sayyidan (Study area) was laid. About 9600 gravity and the same number of magnetic stations were observed in Wad Sayyidan.

One magnetometer was placed at established base station in each area on Auto mode at 60 seconds to control the diurnal variations for observed magnetic data. Normal Correction (N-S & E-W) is also applied for correcting data.

3.4.3 Instrument Used

Following instruments were used in Magnetic data observation:

3.4.4 G-856 Proton Precession Magnetometer

Local magnetic field intensity is calculated by using a magnetometer. The G-856 Proton Precession Magnetometer (Geometrics 856) makes a hydrogen rich fluid (like kerosene) surrounded by an induction coil to generate a strong magnetic field (Gearhart, 2013). Subsequently, the spin axis of the hydrogen protons polarizes with the newly applied magnetic field.

The protons begin to align themselves along the Earth's magnetic field at particular frequency (proportional to the surrounding magnetic field intensity) after the current causing the polarizing field is interrupted (Lenz, 1990).

This precession phenomena induces an alternating current in the induction coil which was previously being used for the generation of the polarization field (Lenz, 1990). The factor relating the precession frequency of the induced voltage with the earth's magnetic field strength is termed proton gyro-magnetic ratio and has a value of 0.042576 Hz/nT. The G-856 magnetometer can be used as a gradiometer with two sensors, or for automatic value recording at the base station (Jeng et al., 2003). Its storage capacity reaches up to 5000 observations with single senor and 2500 with two sensors. G-856 portable man conveyed proton parade magnetometer of Geometrics was utilized to observe the magnetic intensity at the observation stations as well as at the base station (Fig. 3.3).

It gives a precise value of up to 0.1 gamma in normal conditions and 1 gamma in case of supreme conditions. It has a gradient tolerance of 1800 gammas/meter. The instrument was calibrated at the established base station by setting its clock, inputting the Julian date, and tunning the instrument in accordance with the regional magnetic field from the international standard Total MagneticIntensity map. The software used for the data transfer and editing is MagMap2000.

Fig. 3.3: G-856 Geometrics Proton Precision Magnetometer used for magnetic data acquisition.

3.4.5 Hand-held GPS

The Hand-held GPS (Garmin) (Fig. 3.4) was used for the determination of the coordinates for location, survey direction of observation points and for VES Probe Sites and Current Electrode locations in UTM using the WGS84 datum (Odera and Jatani, 2017).

Fig. 3.4: Garmin hand-held GPS used to determine the coordinates of the observation stations.

3.5 Gravity Measurements

In Gravity prospecting, local vertical gravity acceleration is measured. The standard CGS units are Gal (after Galileo) and is equal to the acceleration of 1 cm/sec/sec. The gravitational measurements are the function of mass of geological bodies (LaFehr, 1991). In gravity survey the target is to measure local effect, although gravity measurements at certain point are combination of body directly underneath that point and whole body of earth.

Gravity observations can be described as the measure of density contrast with the surroundings and can be represented as excessive or deficit of mass. After the data is corrected for non-geological effects, it represents the variation of density in earth, especially the lateral contrast. Data processing techniques are applied to separate the local and regional gravity effects.

3.5.1 Detailed Gravity Survey

Detailed Gravity survey was carried out in Wad Sayyidan on grid pattern with 50m profile/line distance and 50m distance between every station.

3.5.2 Equipment and Field Procedure

Autograv CG-5(Scintrex) Gravimeters was used to carry out the detailed gravity survey. The specification of instruments is as follow:

i. Autograv CG-5

CG-5 Autograv gravimeter (by Scintrex) was utilized, which has an accuracy having 1 mgal and shows a residual drift of 0.02mGal/day (Manual, C. G. 2009), to gauge the relative gravity variety in examination area. A tripod is used to level the CG-5 to minimize the error caused by the tilt in the spring of the instrument.

The instrument has fiber made up of quartz with an attached senor that guarantees the estimation goal and can be adjusted up to 1 mgal (Manual, C. G. 2009). It has numerous applications that incorporate salt arch planning, basement rocks, and structural analysis (Robinson, 1988). It can store 0.2 million noticed gravity esteems. Picture of the instrument is as per the following in Fig. no.3.5.

The local bases were tied with the base station at Mandi Bahauddin (g=979.4012 cm/sec^2) and all the gravity data is reduced on this base which is connected with base station at Karachi Airport having absolute gravity of 978.9630 gals (Farah & Ali, 1974).

A regular grid pattern was adopted to cover the areas. The grid spacing in Wad Sayyidan area was 50 x 50 meters. Total Gravity observations in Wad Sayyidan area are 9600. The elevation of gravity measurements was observed with Topcon, topographic surveying instrument and reference elevation was determined from benchmark on the Chenab River Railway Bridge.

Fig. 3.5: CG-5 Scintrex Autograv gravimeter used for the gravity data acquisition.

3.5.3 Establishment of Base Station

There are two types of study to obtain our objective either absolute study or relative study. In absolute study it is a normal requirement of a gravity survey that it should have at least one alreadyestablished gravity base station with its completely determined and known location, absolute gravity value and height with respect to mean sea level. If there is no facility of gravity base station, then gravity base station

must be established by looping unknown base station in a study area witha known base outside the study area ensuring that the looping time is less than two hours in orderto have rigid control over the gravimetric drift.

It is also necessary to establish an auxiliary station at a convenient location in the project area so that any observed gravity loop in the area can be under taken with reference to any of these bases, restricting the looping time within two hours limit. A geographically preserved base station is crucial for an efficient survey (Reudink, Klees et al. 2014). In the present case, relative study has been performed in which a base station was established in the study area for measurement of relative gravity values. and it was not looped with any other establishedinternational gravity station because there was none in the vicinity and outside in the range of thatstudy area.

In general, relative measurement has the advantage of being cheaper, easier than absolute study, and provides sufficient information. So, all the measured value of gravity and magnetic was tied up to the base station which was established in Gali jagir village. The latitude and longitude of the base station are 33.43781 degrees North, and 72.61923 degrees East respectively, with an elevation of 511 meters from mean sea level. Magnetically, it was a quiet location making it suitable for developing a magnetic base station.

3.6 Electrical Resistivity

The resistivity of a specimen is the ability of material to resist the flow of electric current (Kearey et al., 2002). Flow of electric current is governed by Ohm's Law (Herman, 2001). Ohmic resistance of a unit volume of a material is called the electric resistivity. The electrical resistivity survey measures the electrical potential, which is developed when a current is passed through the body. Two electrodes are used to transmit an electric current into the earth (Herman 2001).

The flow of current develops a potential difference which is measured using porous pots. The electrical Resistivity of rocks and minerals depends upon a number of

factors like porosity, degree of saturation, pore electrolytes and conducting properties of rock matrix. Minerals have metallic luster and their minerals are good conductors.

Crystalline rocks normally have high resistivities but sometimes may vary to low in the presence of conducting minerals like magnetite, graphite etc. The measured resistivity is said to be true if the measurement is done over an isotropic, homogenous, finite space. If, however, the measurement is done over an anisotropic and inhomogeneous medium, the measured values are termed as apparent resistivity.

Electrical resistivity measurements are executed in two ways, either for depth soundings i.e., VES, or profiling. In depth soundings measurements are made at different electrode spacing at a single point, while profiling involves data acquisition at different stations along profile or over an area keeping same spacing. VES survey has been carried out in Wad Sayyidan area for detailed investigations.

3.6.1 Induced Polarization

IP measures the potential field induced into the ground for mapping geological subsurface (Sumner, 2012). The induced current often takes time to deteriorate after switching off the current. This method plays a significant role in delineating both massive as well as disseminated ores. Another form of IP method is the time domain method which quantifies the chargeability and voltage decay over a specific interval of time after the current is switched off (Sumner, 2012).

An IP survey is similar to resistivity because to carry out IP one has to inject current into the ground and measure potential difference that exists shortly after the current is switched off. As with resistivity, the current direction is reversed at intervals to average out any steady potential present (mainly due to self- potential or telluric currents).

The results of an IP survey are usually expressed as Chargeability in time domain. The IP surveys involve little data processing and interpretation. Often nothing more than plotting the values of the chargeability as a profile, pseudo section or on a grid is required for interpretation (Dahlin et al., 2002).

3.6.2 Field Procedure

The aim of the survey was to measure the resistivity of subsurface and chargeability of the area for expected conductive and sulphide mineralization. Schlumberger Electrode Configuration was used to map the areas of Wad Sayyidan on profiles.

The depth of investigation was 1000 meters. IP values (i.e., chargeability) is measured along with Resistivity at each spacing. The orientation of each VES was kept constant and perpendicular to the strike of the inferred subsurface structures. The following spacing for Current and Potential Electrode was used in table no. 3.1.

Table. 3.1: Represents the spacing used for current electrodes AB/2 and potential electrodes MN/2.

AB/2	MN/2	AB/2	MN/2	AB/2	MN/2	AB/2	MN/2
10	2	80	2/10	300	10/50	700	50
20	2	100	2/10	400	10/50	800	50
40	2	150	10	500	50	900	50
60	2	200	10	600	50	1000	50

When the MN/2 increased, two simultaneous readings were observed at the same distance to confirm the accuracy. A total of 55 Resistivity/IP soundings were executed in the study area Wad Sayyidan to the depth of 1000 meters.

3.6.3 Instrument Used

The following instruments were used for electrical resistivity survey:

3.6.4 Resistivity Transmitter

TSQ-3 Transmitter of Scintrex was used for ground energizing in fig. 3.6. Specifications of transmitter are discussed as follows in Table 3.2.

Table. 3.2: Table represents the specifications of resistivity transmitter.

Sr.no.	Power	Range
1	Output power	3000 VA maximum
2	Output Voltage	300 to 1500 volts selectable in 9 discrete steps
3	Output Current	10 amperes maximum

Fig. 3.6: TSQ-3 Scintrex Resistivity Transmitter is used to control transmission of electric current to current electrodes during resistivity/IP data acquisition.

3.6.5 Resistivity Receiver

IP Receiver (IPR-12) and RDC-10 of Scintrex, were used for survey. The specification of each receiver is as follows:

i. IPR-12 Resistivity Receiver

IPR-12 has multiple outputs allowing from one to eight multiple dipole measurements with Input Voltage Range: 50µV to 14V, Chargeability:0 t0 300 mV/V, Absolute Accuracy: Better than 1%, Vp Integration Time: 10% t0 80% of the current on time and Reading Resolution of Vp, SP and M are10µV, 1mV and 0.01mV/V respectively as shown in fig. 3.7.

Fig. 3.7: IPR-12 Scintrex IP/Resistivity Receiver is used to calculate the value of chargeability and resistivity during resistivity/IP data acquisition.

ii. RDC-10

In order to measure the potential difference, the Resistivity Receiver RDC-10 (Scintrex) was used. This instrument can measure primary voltage in 12 ranges from 30 microvolt to 30 volts as in fig. 3.8.

Fig. 3.8: RDC-10 Scintrex Resistivity Receiver is used to calculate the value of resistivity during resistivity data acquisition.

3.6.6 Resistivity Generator

Resistivity generator supplies 220 volts AC output for step up transformer in the transmitter, for maximum 1500 volts DC input ground current. Resistivity generated with all the required instruments is shown in fig. 3.9.

Fig. 3.9: Resistivity Generator along with all necessary instruments used for carrying out the resistivity/IP data acquisition profiles.

CHAPTER NO. 4

DATA PROCESSING
(Magnetic, Gravity & Resistivity/IP)

4.1 Magnetic Data Processing

During magnetic data processing the following two corrections were applied to the magnetic data.

4.1.1 Diurnal Correction

The Geomagnetic field varies within short periods of time of the order of hours due to the movement of ionic clouds in the ionosphere. These variations are called diurnal variations and to correct for these variations, diurnal-correction was applied by reoccupying the base station (Dentith and Mudge, 2014).

4.1.2 Normal Correction

Since the geomagnetic field is a bi-polar field, therefore the magnetic field also varies in the north south and east-west direction, i.e., as we move from equator to poles, the field increases. Therefore, to account for this variation, normal-correction is applied; a value of 4.3 nano Tesla/km along N-S direction and 1 nano Tesla /Km was used for this purpose (Total Intensity Map of the World, U.S. Naval Oceanographic Office, 1990) (Dentith and Mudge, 2014).

4.1.3 Data Presentation

Magnetic data is reduced on the local bases for semi-detailed and detailed magnetic survey and 2-D surfer contour maps, profiles and cross sections are prepared by using the Software “Surfer11” after applying the Diurnal and Normal Corrections for the Wad Sayyidan area.

4.1.4 Residual Anomaly Map

To enhance magnetic effect of local anomalous zone, Grid Residual was computed by computer programme in GW-Basic language (Javaid, 2002) using

Griffin's 9-point-two-ring formula (Dobrin, 1981, Telford, 1984) with different average ring radius for each area. The Griffin's formula is given by Eq.4.1.

$$R = G_0 - \left(\frac{SUM}{8}\right), \qquad \text{Eq. 4.1}$$

where, G_0 = the magnetic value at the central point of rectangular 9-point cell on grid, SUM = Sum of 8 magnetic points around two circles. The magnetic data after necessary corrections have also been plotted on 2D contour maps by using SURFER (Version 11).

4.2 Gravity Data Processing

4.2.1 Rock Density

The value of density is required to calculate the Bouguer Correction which compensates for the material within the elevation of observed station and the datum. The density of 1.8 gm/cc has been used for alluvium. The average density of basement rocks consisting of Quartzite, Granite, Schist, Quartose Schist etc. is 2.7 gm/cc (Aziz ur Rehman 1963).

4.2.2 Reduction of Gravity Data

Reduction of observed gravity values was performed in accordance with the base station value. The bases were connected with the Mandi Bahauddin gravity base. The local bases in the area were periodically re-occupied to minimize the effect of drift of gravity meters. The location of base in study area is, Wad Sayyidan 72.94284402˚ Easting 31.81749461˚ Northing.

The data of each area was processed by applying instrument drift, free air, Latitude and Bouguer Corrections.

4.2.3 Latitude Correction

Earth is not a perfect sphere as its equatorial radius is greater than polar radius. Therefore, gravity increases from equator to poles irrespective of subsurface geology (Hinze et al., 2013). Hence, the variation in gravity is the function of Latitude. For

latitude correction, International Gravity Formula (IGF-1980) was used to correct the data for latitude corrections. The IGF-1980 formula is given by Eq. 4.2.

$$g_o = 978032.7(1 + 0.0052790414Sin^2 * \lambda + 0.0000232718Sin^4 * \lambda + 0.0000001262Sin^6 * \lambda), \quad \text{Eq. 4.2}$$

where, g_o is referred as theoretical gravity or normal gravity and λ is geographic latitude of station observed.

4.2.4 Free Air Correction

Since gravity decreases as we move away from center of earth (i.e. elevation increases). Therefore, Free Air correction is applied for correcting the data of each station to account for the gravity variation due to change in elevation (LaFehr, 1991). The elevation of local base station in Wad Sayyidan is 183.40 meters.

The above-mentioned local base was connected with Mandi Bahauddin Base with elevation of 233.88 meters (731.60 ft). The formula for Free Air Correction is given as in Eq. 4.3.

$$F.A = h * 0.3085, \quad \text{Eq. 4.3}$$

where, h is the elevation difference between station elevation and datum.

4.2.5 Bouguer Correction

Bouguer Correction compensates the effect of gravity caused by the material between the base and the station elevation (Dentith and Mudge, 2014). The Bouguer correction is measured and given in Eq. 4.4.

$$g_{obs} = h * D * 0.04188, \quad \text{Eq. 4.4}$$

where, h is the elevation difference between station elevation and datum, D is the density, 1.8 gm/cc was used for processing data. In general, if observed point elevation is less than that of base (datum) then this correction will be negative and vice versa.

The combination of Free Air and Bouguer Correction is called as Elevation Correction. The sign of these corrections is always opposite (i.e., if one is positive than the other will be negative).

4.2.6 Terrain Correction

There is no appreciable variation in terrain in the areas under investigation or in close proximity, therefore, terrain correction is not applied to the data.

4.3 Accuracy of Data

The accuracy of data is calculated by estimating the magnitude of observational and computational errors in application of different corrections to field gravity data. The drift of gravity meters used in survey is summarized as in table.4.1.

Table.4.1: Gravimeter used in Wad Sayyidan

Gravity meter	Serial No.	Model No.	Drift (mgals per hour)
Autograv (CG-5)	050600128	CG5	0.032

4.3.1 Residual Anomaly Map

To enhance the gravity effects of smaller and weaker anomalies, Grid Residual was computed by computer programme in GW-Basic language (Javaid, 2002) using Griffin's 9-point-two-ring formula (Dobrin, 1981, Telford, 1984) at different average ring radius for each area. The Griffin's formula is given in Eq. 4.5.

$$R = G_0 - (\frac{SUM}{8}), \qquad \text{Eq. 4.5}$$

where, G_0 is the gravity value at the central point of rectangular 9-point cell on grid, SUM is the sum of 8 gravity points around two circles.

By comparing the Bouguer Anomaly map with the Residual Anomaly maps at different average ring radius, the smaller and weaker anomalies can be easily identified. The deeper structures or bodies in the subsurface produce the broader and weaker anomalies which are not apparent on the Bouguer Anomaly map.

The gravity data after necessary corrections and reduction to base have been plotted on 2-D contour maps by using Surfer (Version 11).

4.3.2 Gravity Anomalies

As a result of successive application of the above corrections, the following gravity anomalies canbe sequentially obtained for each observation.

i. Free Air Anomaly
ii. Bouguer Anomaly

i. Free Air Anomaly

Free air anomaly (F.A.A) was generated when Latitude correction (L.C), Drift correction (D.C) and Free Air Correction (F.A.C) have been applied on the observed gravity value. Free air anomalyis defined as in Eq. 4.6.

$$F.A.A = G_{obs} \pm L.C \pm D.C \pm F.A.C - G_{thg} \quad \text{Eq. 4.6}$$

Any Free Air Anomaly map will generally show a strong correlation with local topography.

ii. Bouguer Anomaly

The Bouguer anomaly compensates for the lateral density variation in the subsurface which causes a difference in the observed and the absolute gravity value at any station (Ervin, 1977). An allocation was made due to the change in gravity with height, latitude, and due to the topography, these corrections are called bouguer, latitude, free air, and terrain correction.

All of the preceding corrections have been applied to the observed gravity readings, the value of bouguer gravity anomaly for the station was obtained as in Eq. 4.7.

$$g_B = g_{obs} \pm d_{gL} \pm d_{gF\cdot A} - d_{gB} + d_{gT} \quad \text{Eq.4.7}$$

where, g_{obs} is field station reading, d_{gL} is latitude correction, $d_{gF\cdot A}$ is free air correction, d_{gB} is Bouguer correction, and g_{gT} is terrain correction.

The Bouguer Anomaly is given in Eq. 4.8 as:

$$\rho * g_B = g_B - g_r \quad \text{Eq. 4.8}$$

where, g_r is particularly station value in the survey area.

4.4 Resistivity/IP Data Processing

4.4.1 Processing & Modeling of Resistivity and IP data

For the processing and modeling of VES curves software "IPI2WIN" of Moscow University was used. Simulation of actual subsurface configuration of the lithological units was done by getting the best fit of the observed and calculated curve with a minimum Error % (Gupta et al., 1997). The interpreted curves gave a most plausible subsurface model simulating the actual lithological setup occurring at the probe sites.

For IP data the cross-section along profiles are prepared and also generated 2-D maps of Chargeability at different horizons like 100, 200, and 300 to 1000 meters. Similarly, apparent Resistivity 2-D maps are also prepared at these horizons for comparison using contouring software "Surfer 11".

CHAPTER NO. 5

INTERPRETATION
(Magnetic, Gravity & Resistivity/IP)

5.1 Introduction

Interpretation is the route toward examining data through some predefined measures which will help consign some noteworthiness to the data and reach a significant conclusion result. It incorporates taking the eventual outcome of data assessment, making inducing's on the relations considered, and using them to close.

Data interpretation techniques are the methods by which investigator help to sort out numerical data that has been assembled, analyzed and presented. Data,when accumulated in unrefined structure, may be difficult for the layman to appreciate, which is the explanation specialists need to isolate the information amassed so others can sort it out.

A good interpretation needs to be consistent with the background knowledge of our study area, not only the geological significance is to be accounted for but other auxiliary data including well information, previous literature and any work done needs to be accounted for when interpreting the data to obtain consistent results of tracing out anomalous zone in our models.

Interpretation consists of two types, namely qualitative and quantitative, with the meaning of the terms explained as follows:

- The qualitative data interpretation strategy is utilized to investigate qualitative data, whichis otherwise called all out information.
- The quantitative information interpretation technique is utilized to dissect quantitative information, which is otherwise called mathematical information.
- This information type contains numbers and is accordingly investigated with the utilization of numbers.

5.2 Regional View of The Area

The total area of 28 toposheets show a division of low and high magnetic. The division is elongated in NW-SE direction initiating from 43D/16, 44E/1, 44E/6, 44E/11, 44E/16 and 44I/4. The NW-SE elongated contours are probably the signature of subsurface concealed fault with different depths of basement rocks on the both sides of inferred fault or may be due to no significant change in depth due to the presence of different types of rocks (Fig.5.1).

A number of drill holes data is available on the southern side of this inferred dividing line like Chiniot, Rajoha, Wad Sayyidan, Ghutti Sayyidan, Chak Jhumra etc. However, GSP has only the data of Chiniot area which was drilled by GSP in 1990s. The drilling data which was recently carried out by PMC, was not available. The anomaly of Chiniot iron ore is present in toposheet No. 44A/14. Similarly, Ghutti Sayyidan anomaly is also present in the same sheet.

The other two anomalies covered during current exploration program are Wad Sayyidan in the NNW of Chiniot in toposheet No. 44A/13 and Chak Jhumra anomaly in toposheet No. 44E/2. Different amplitude of magnetic signature on opposite side of the inferred concealed fault is observed with cumulative low on the southern part and relatively high on the northern part of the area.

The magnetic anomaly of Chiniot and other three investigated areas lie on the southern side of inferred concealed fault. Number of rocks exposures are present in this part with Kirana hills, Chiniot and Sangla hill etc. The rock types in the area are meta-sedimentary which include quartzite, slates and phyllites and the igneous rocks include lava flow, volcanic breccia and tuffs, basic intrusive rocks etc.

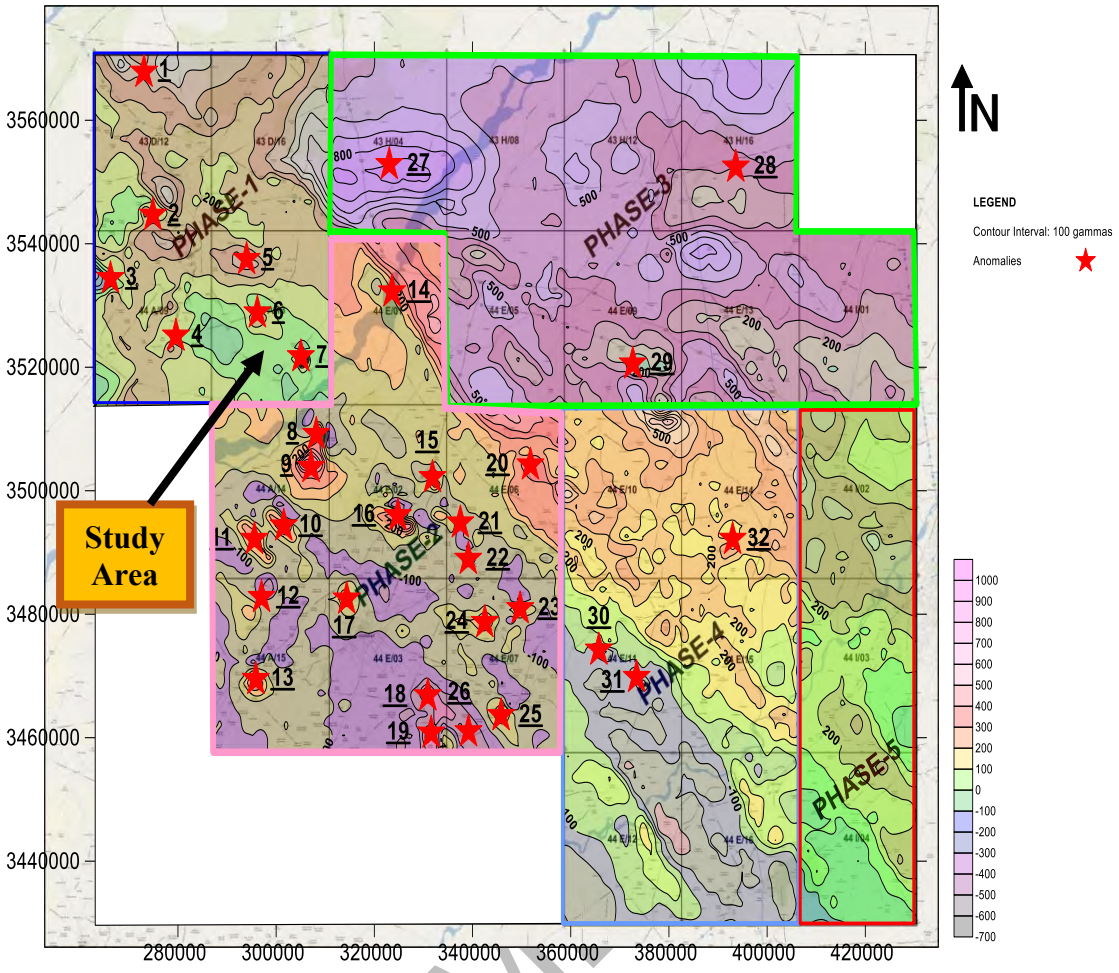

Fig. 5.1: Map representing the Total Field Magnetic Anomaly Map of 28 Toposheets with red star mark Showing Anomalous Zones including study area which is marked toposheet no. 44-A/13 Wad Sayyidan.

5.3 Semi-Detailed Magnetic Survey Interpretation of Topo Sheet No. 44A/13

This region (Fig. 5.2) contains scattered outcrops along with three anomalous zones near Kot Qazi, Lalian and Sharaban Hill. Northern part of this map shows comparatively moderate to high magnetization and lower part shows low magnetic zone oriented in a NW to SE direction. This low magnetic intensity zone is likely to be caused by the presence of meta-sediments at shallow depth under the alluvium. The anomaly of Sharaban area lies in the moderate to high intensity zone whereas the anomaly of Kot Qazi and Lalian lies along the low magnetic intensity zones. Out of these three anomalies sites (Table 5.1), Kot Qazi found most promising and recommended for

detailed Integrated Geophysical Survey, whereas two other sites are recommended for gravity profiles.

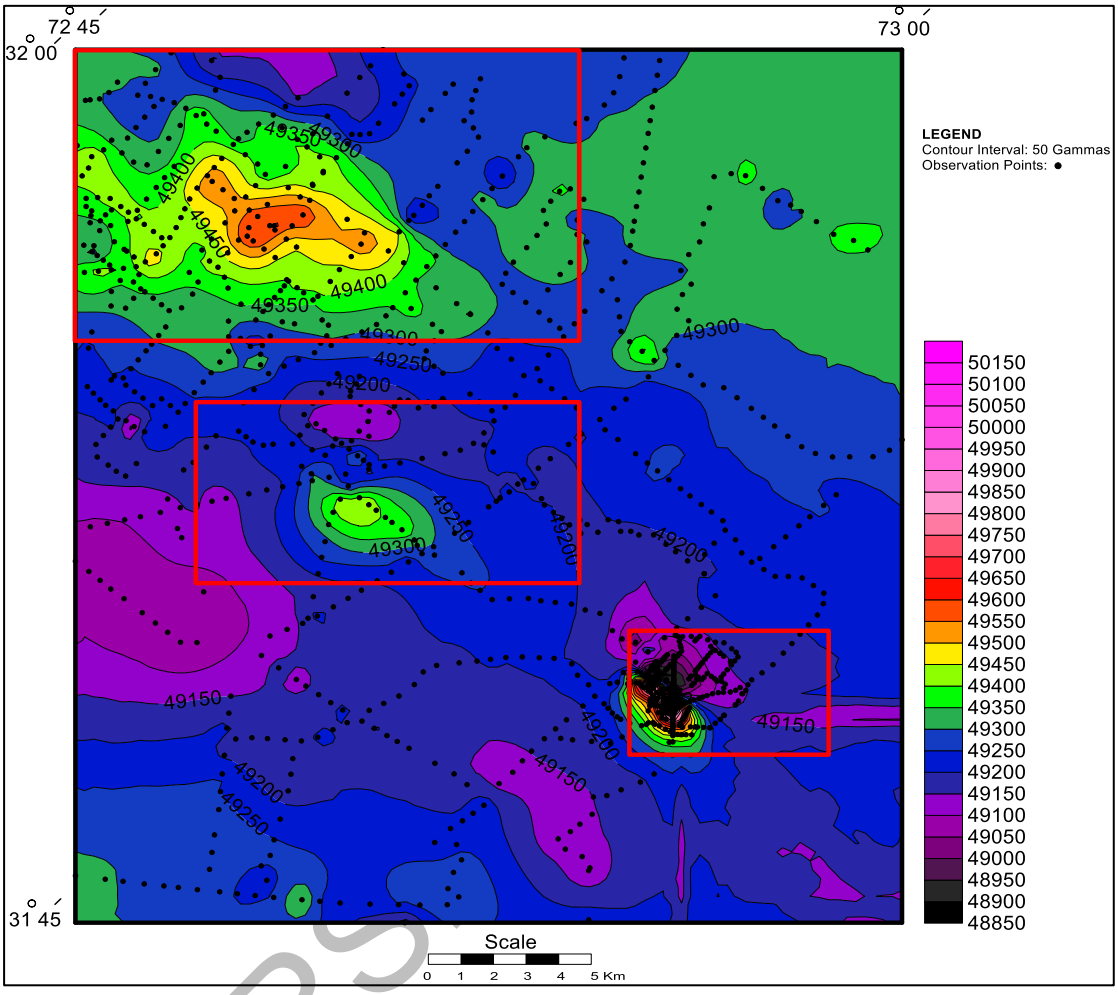

Fig. 5.2: Total Intensity Magnetic anomaly map of the Toposheet no. 44-A/13 showing 03 anomalous zones highlighted by red rectangles.

Table. 5.1: Anomalies Recommended for Detailed Integrated Geophysical Survey. The areas recommended by location (UTM) in the following Anomalous zones for Detailed Integrated Geophysical Surveys may vary depending upon the lateral extent of the anomalies after applying different Geophysical Methods.

Sr. no.	Phases	No. of Anomalies	No. of Sheets	No. of Anomalies per Sheet	Coordinates of Anomalies
1	Phase-I	03	44-A/13	03	i. 287150E 3533200N ii. 304150E 3719950N iii. 290850E 3525440N 302580 E 3542440 N 310210E 3523900N 302585E 3531200N

5.4 Detailed Integrated Geophysical Survey Interpretation (Gravity, Magnetic & Resistivity/IP)

WAD SAYYIDAN

Gravity, Magnetic and IP/Resistivity methods were used in the area as integrated geophysical survey.

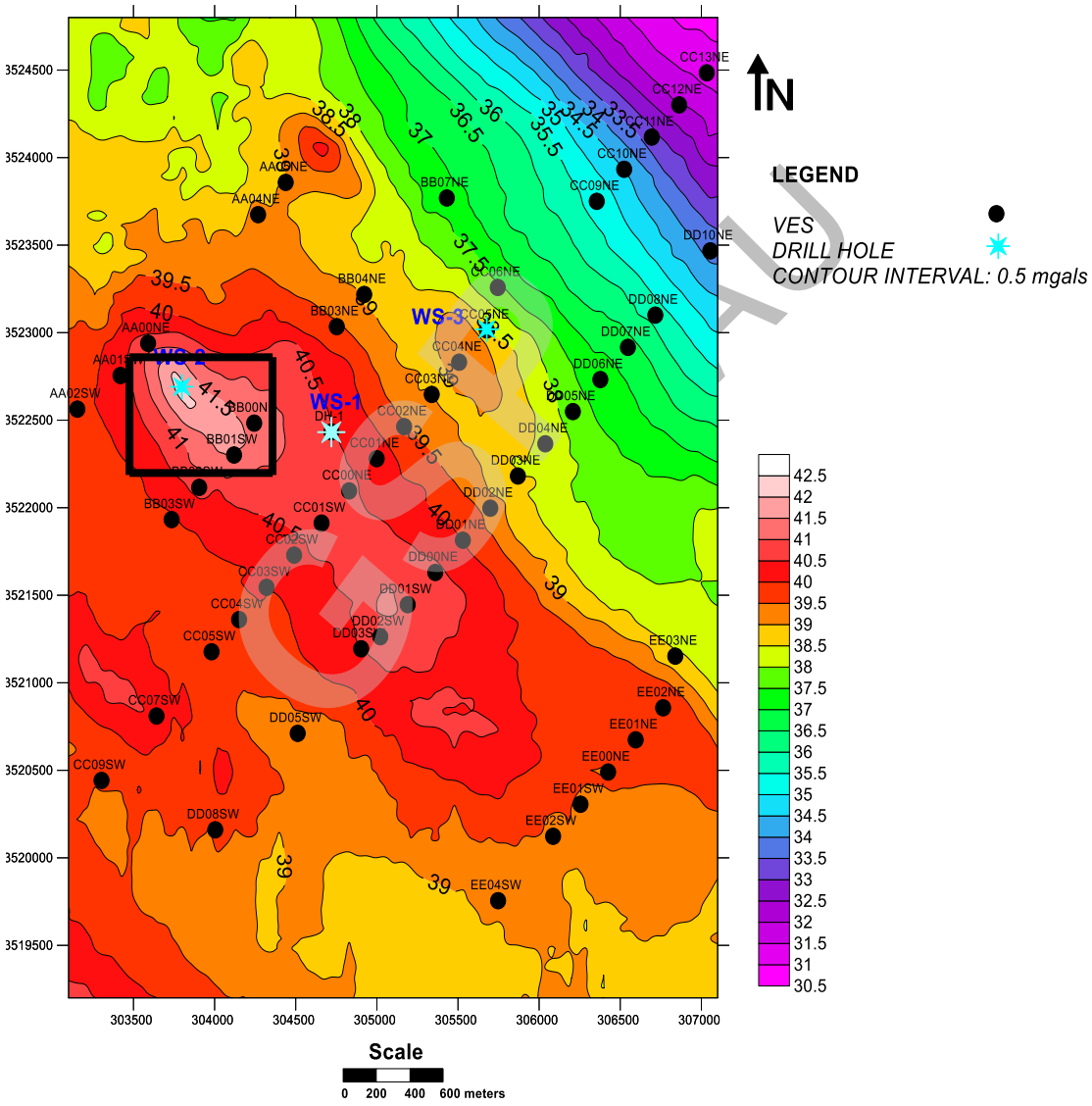

Fig. 5.3: Bouguer gravity anomaly map of Wad Sayyidan Area shows an ascending trend of gravity signature from Northeastern corner of the map towards center, where highest bouguer gravity behavior with peak contour of 42 mgals is observed marked with black rectangle.

5.4.1 Bouguer Gravity Anomaly Map

Bouguer gravity anomaly map in Punjab Plains normally reflects the subsurface topography of the basement rocks. However, the existence of some magnetic anomalies also warrants the appearance of magnetic susceptible materials like magnetite. The total variation in the Wad Sayyidan area is 11 mgals (Fig. 5.3).

The Bouguer gravity anomaly map shows the contour trend of Northwest to Southeast direction, supporting the magnetic trend observed in the semi-detailed magnetic survey of the area. There is an ascending trend of gravity signature from Northeastern corner of the map towards center, where highest bouguer gravity behavior with peak contour of 42 mgals is observed, align in NW-SE direction.

The map exhibits the concealed fault in the close proximity of the highest anomaly on the NE side following the regional behavior of magnetic signature. Two distinct, with smaller lateral extent of high bouguer gravity zones are also present in the northern half of the map. High gravity signature in the NW corner of the mapped area corresponds to the presence of small rock exposures in the cultivated lands.

The exposed rocks showing the presence of iron mineralization like Specularite (black metallic crystals). The small rock exposed in the area and generating the higher bouguer gravity signature supports the general concept of subsurface basement topography in the Punjab plains.

The central highest bouguer gravity anomaly (42 mgals) with larger lateral extent and no rock exposures in the zone probably leading towards the presence of some high-density material in the subsurface. A gentle decreasing trend of gravity behavior is observed towards SW direction from the center of map.

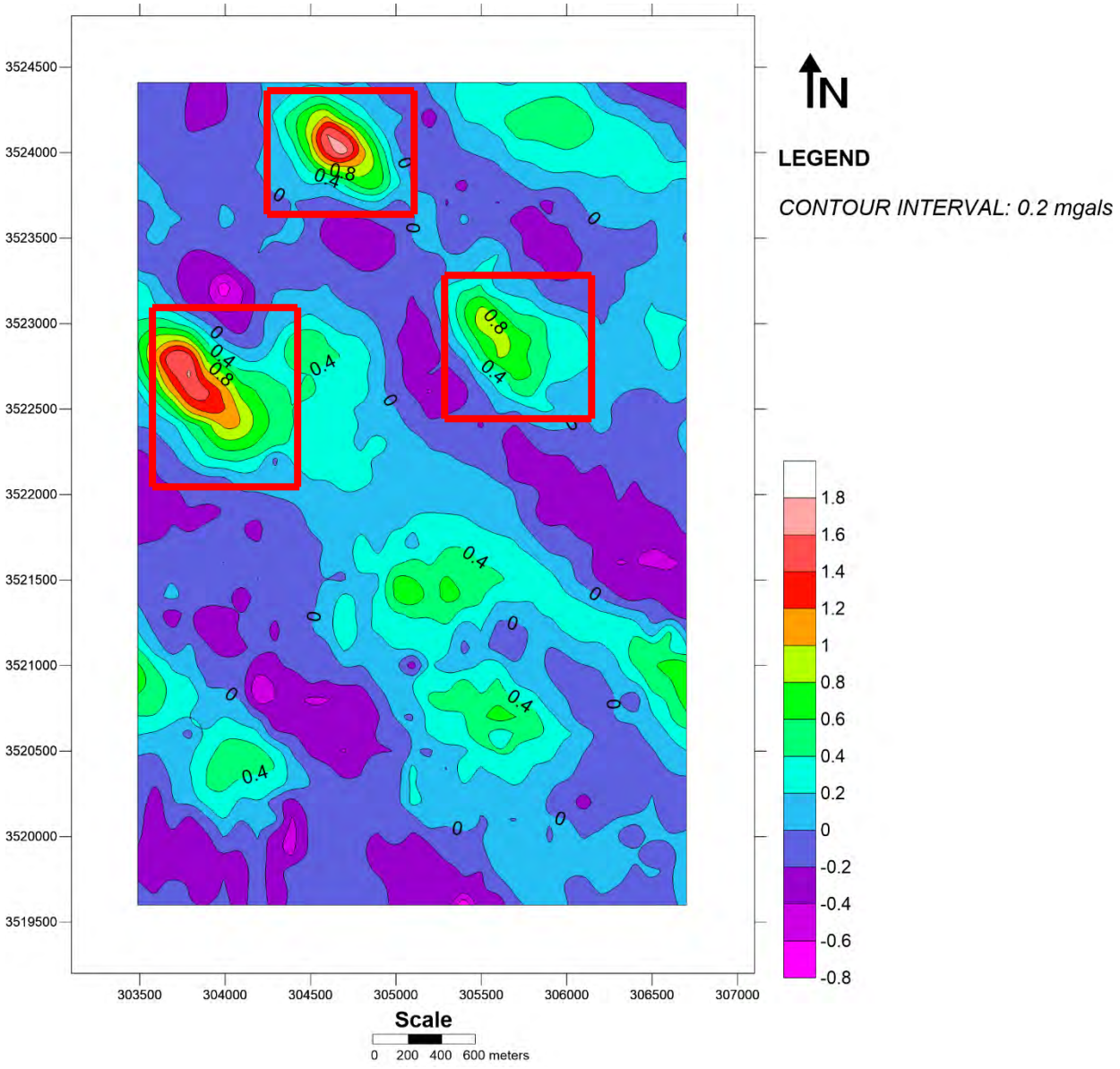

Fig. 5.4: Residual Bouguer Gravity Anomaly Map of Wad Sayyidan Area enhance the local effect by subtracting the regional part of Bouguer Gravity. Three distinct anomalies are evident in the Residual Bouguer Gravity Anomaly map marked by red rectangles. (Average Ring Radius=482 meters)

5.4.2 Residual Bouguer Gravity Anomaly Map

Residual Bouguer Gravity Anomaly Map is prepared at an average ring radius of 482 meters by Griffin's method. The aim of the residual map is to enhance the local effect by subtracting the regional part of Bouguer Gravity. Three distinct anomalies are evident in the Residual Bouguer Gravity Anomaly map (Fig.5.4).

The main Bouguer Gravity Anomaly is shrinking by lateral extent with amplitude of 1.6 mgals at the western side in upper half of the map. Another anomaly at the top portion of the map is also comparable with the main anomaly with amplitude of 1.6 mgals and it corresponds to the small exposure of basement rocks in the cultivated lands. Generally, the bouguer gravity anomalies in Punjab Plains follow the subsurface topography of the basement rocks.

There are no exposed rocks in the vicinity of main anomaly but producing equal gravity effect with the anomaly where rocks are exposed at the surface, leading towards the presence of some high-density metallic minerals like magnetite in subsurface at the location of main anomaly. Another anomaly with amplitude of 0.8 mgals is present in the Northeastern part of the map with orientation in NW-SE direction.

In the central part of the map main anomaly and two NW-SE trending anomalies on the Northern side of map are separated by negative gravity effect. The negative gravity effect with contour value of -0.2 mgals is comparable with the subsurface concealed fault which is also depicted in VES carried out in Wad Sayyidan area.

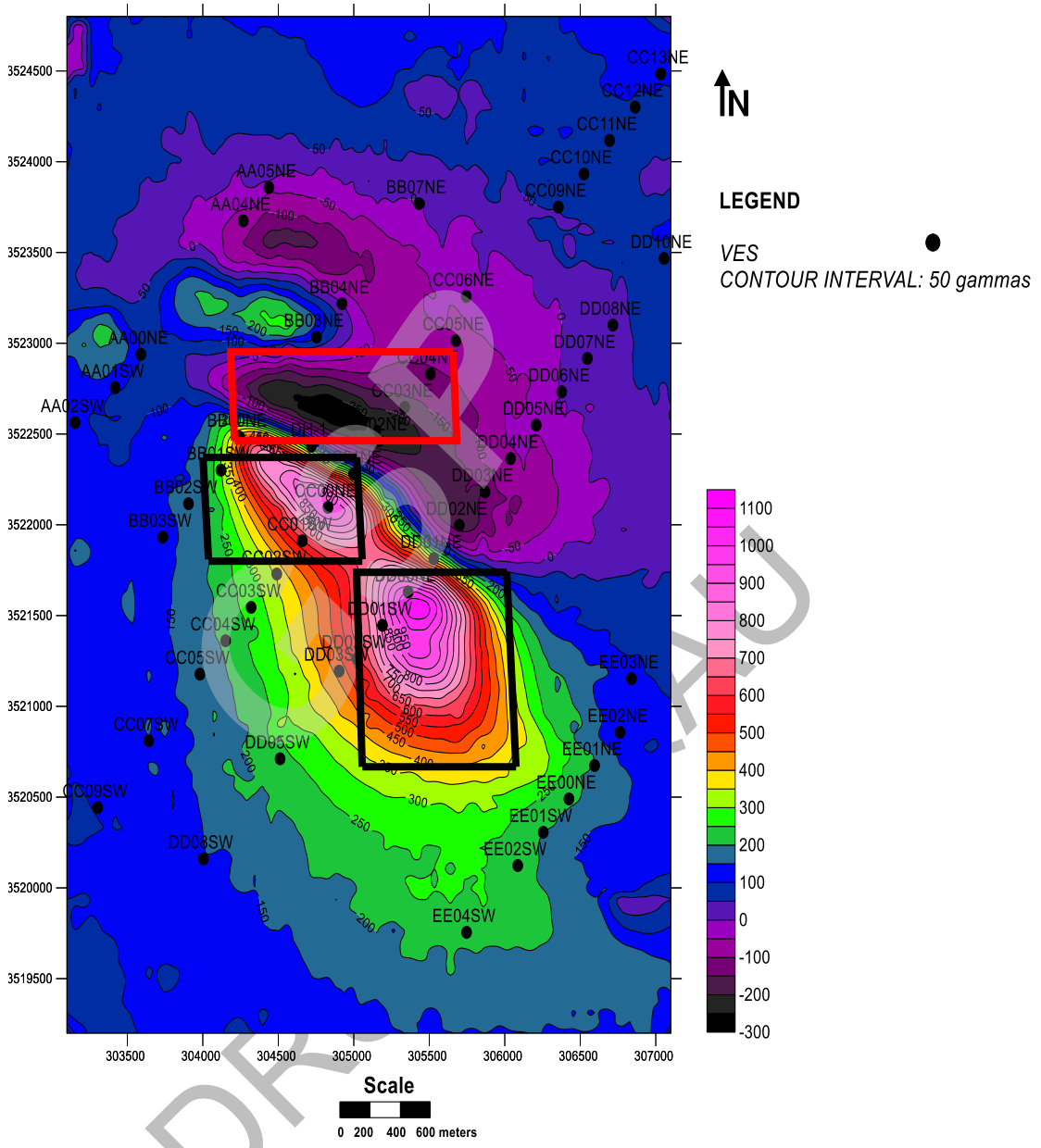

Fig. 5.5: Total Magnetic Intensity Anomaly Map of Wad Sayyidan Area shows normal dipolar magnetization. The magnetic behavior shows two distinct anomalies very close to each other marked in black rectangles. Two positive peaks are present close to each other with one negative peak marked in red rectangle.

5.4.3 Total Magnetic Intensity Anomaly Map

The map shows normal dipolar magnetization with total amplitude of 1400 gammas (Fig.5.5). The magnetic behavior shows two distinct anomalies very close to each other. Two positive peaks are present close to each other with one negative peak with lowest contour of -250 gammas.

The less differentiation of negative peaks into two is probably due to existence of very close proximity of bodies generating the signature. Another magnetic anomaly of 400 gammas amplitude is present in the northern half of the map towards North-West corner with smaller lateral extent.

This anomaly has close correlation with the small exposure of rocks in the area, generating the gravity signature at approximately same location. The main magnetic anomaly trend is NW-SE direction, following the general regional magnetic trend of the area as observed in semi-detailed magnetic survey. The data shows the emplacement of some magnetic susceptible material along the weak zone (fault).

The positive magnetic peak is approximately correlated with the positive bouguer gravity peak. A gentle variation is observed in the mapped area from center on both sides in the background values.

The orientation of the gradient of main anomaly corresponds to the concealed fault delineated in the bouguer gravity anomaly map. The similarity in trend of gravity and magnetic leads toward the existence of same subsurface source generating the signatures.

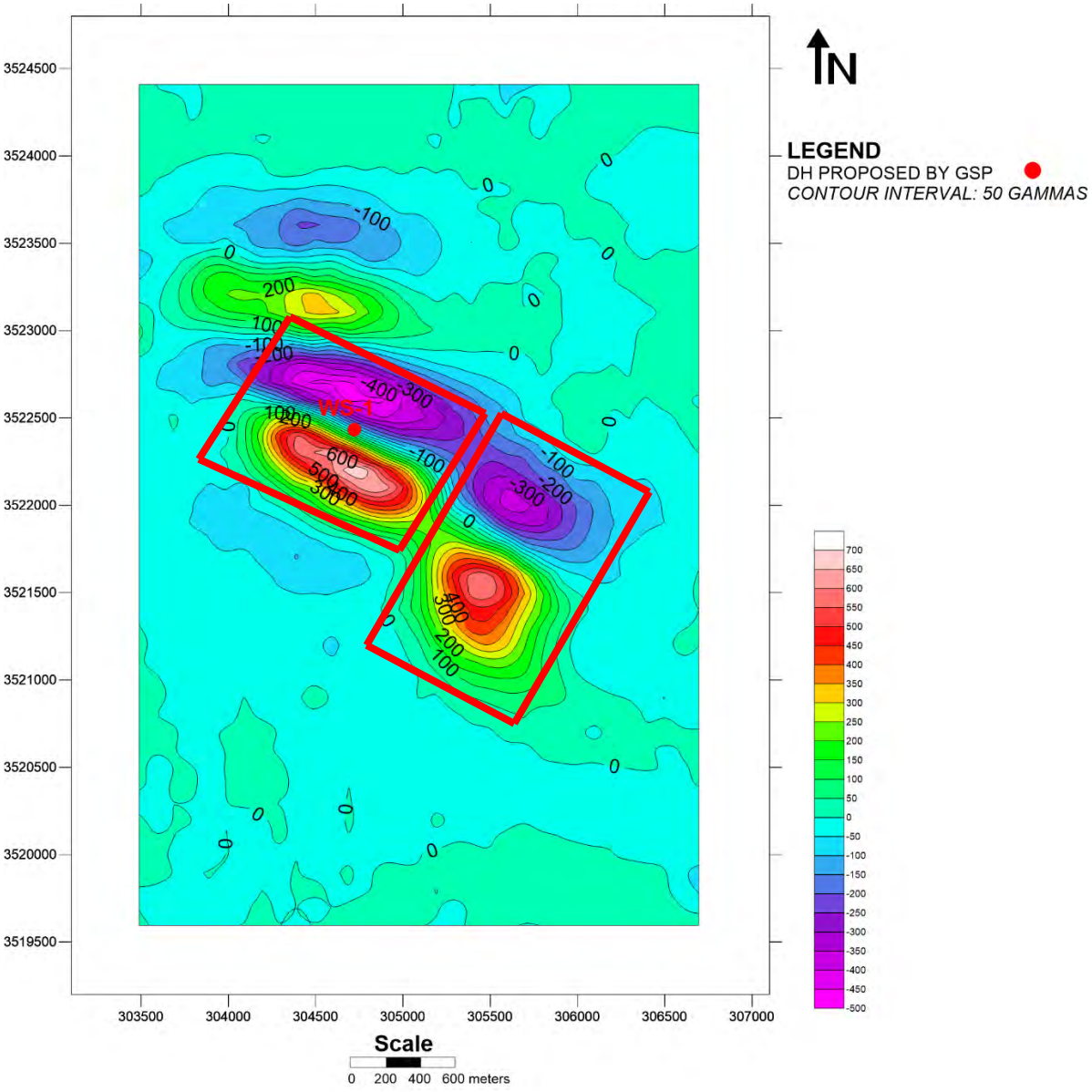

Fig. 5.6: Residual Total Magnetic Intensity Anomaly Map of Wad Sayyidan Area shows two distinct anomalies at the center of the area with NW-SE strike direction marked in red rectangles. (Average Ring Radius=482 meters)

5.4.4 Residual Total Magnetic Intensity Anomaly Map

Residual Total magnetic Intensity Anomaly Map is prepared by Griffin's method at an average ring radius of 482 meters (Fig. 5.6). The map shows two distinct anomalies at the center of the area with NW-SE strike direction.

The amplitude of these anomalies are 1150 and 900 gammas, respectively. Another, relatively low amplitude anomaly of about 500 gammas presents on the Northwestern corner of the map, which is correlated to the small rock exposure in the area. Smooth background behavior is observed throughout the investigated area in residual map.

5.5 VES and IP surveys

5.5.1 Interpretation of Profile AA

The apparent resistivity values vary in the range of 40-300 Ohm-m. In general, three-layer cases are observed with sand after alluvium fill, clays/silt or water saturated sands and then basement rocks continued till the explored depth (Fig. 5.7).

The basement top varies in the range of 127 to 244 meters along this profile. The high resistivity zones at top with small thickness correspond to the dry sand above water table. The chargeability pseudo section shows a continuous and constant behavior in unconsolidated strata comprising of sand and silt/clays with maximum value of 10 mV/V (Fig. 5.7).

However, a continuous increasing trend is observed in basement rocks with depth. A high chargeability zone with maximum value of 42 mV/V is observed at depth of 800 meters on station AA01SW and AA00NE with good correlation of relatively low resistivity in the apparent resistivity pseudo section.

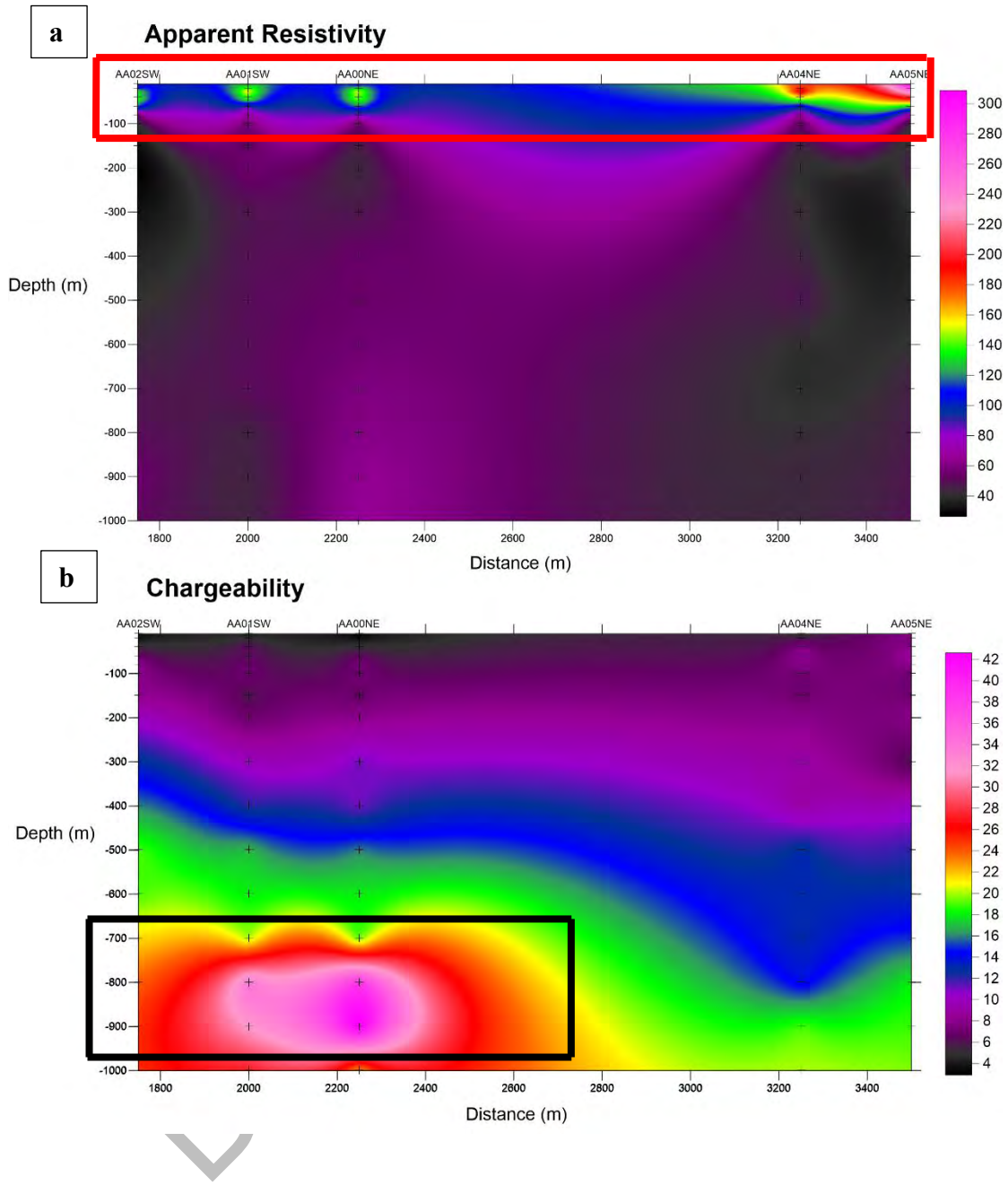

Fig. 5.7: (a) Apparent Resistivity shows high resistivity zones correspond to the dry sand above water table marked in red rectangles. (b) Chargeability Pseudo-sections shows high chargeability zone with maximum value of 42 mV/V is observed at depth of 800 meters marked in black rectangle.

5.5.2 Interpretation of Profile BB

The apparent resistivity variation along this profile is in the range of 20-400 ohm-m. Seven VES/IP points have been observed in the depth range of 500-1000 meters. The sand fill is comparatively high on the Northeastern side of the profile.

Two conductive zones in the depth range of 300 to 400 meters are present at the vicinity of BB03SW, BB02SW, BB03NE and BB04NE, respectively. The depth to basement top varies in the range of 160 meters to 302 meters (Fig.5.8).

The chargeability variations are continuous increasing behavior inside the basement rocks, in general. However, chargeability increases to high twenties in the SW portion of the profile with maximum value of 28 mv/v.

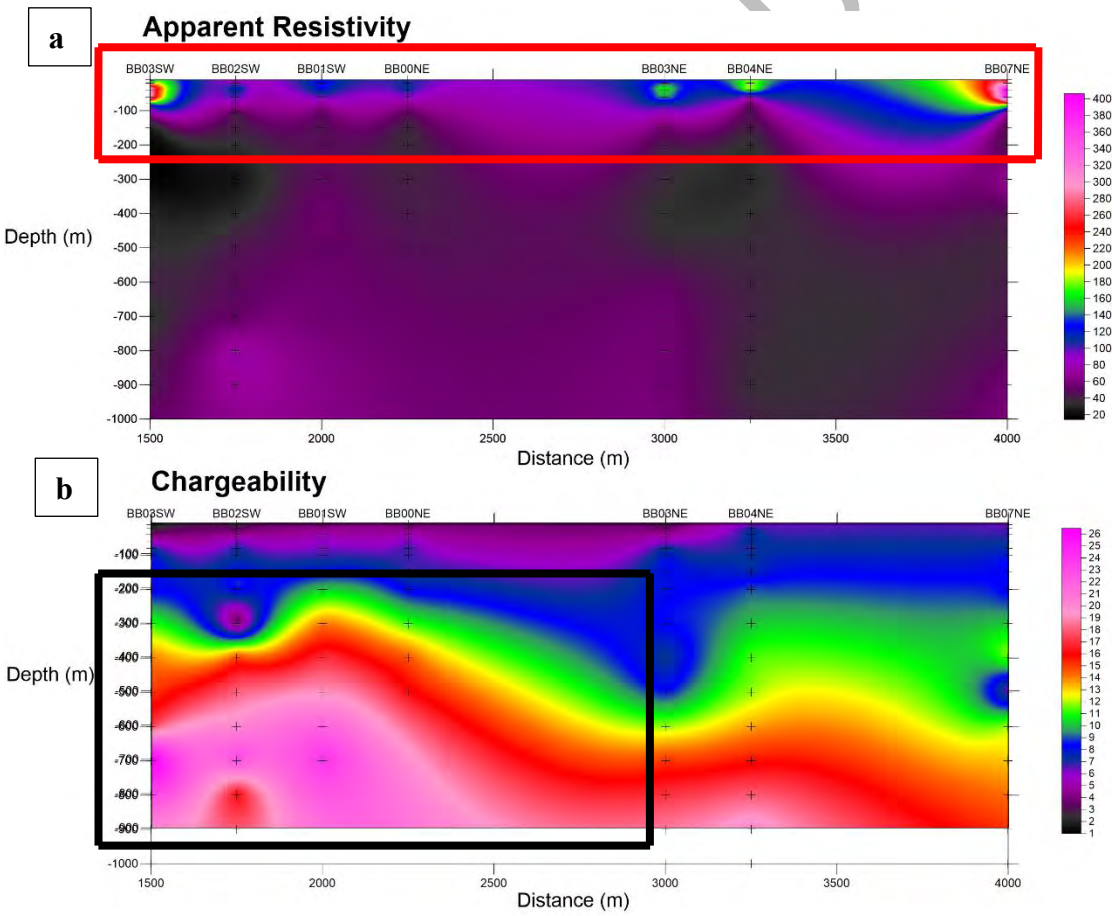

Fig. 5.8: (a) Apparent Resistivity shows variation and high resistivity zones at top with correspond to sand which is marked with red rectangle. (b) Chargeability Pseudo-sections shows chargeability increases to high twenties marked in black rectangles.

5.5.3 Interpretation of Profile CC

A very unique trend of apparent resistivity is observed on number of observation points on this profile. The apparent resistivity values increase in such a manner that could not be matched/modeled with master resistivity curves.

The behavior normally is the signature of presence of subsurface fault/ irregular topography in basement shield rocks in the vicinity. However, the normal curves which could be modeled show a huge variation in basement depth. The presence of dry sand thickness is comparatively high on the observational points CC03NE to CC09NE (Fig.5.9).

The chargeability pseudo section shows a high chargeability NE dipping Zone on point CC04NE to CC06NE. A constant behavior of chargeability in the range of 5-15 mv/v is observed throughout the investigated depth along the profile. The zone of high chargeability indicates the probable presence of sulphide mineralization at the contact of basement rocks and metasediments.

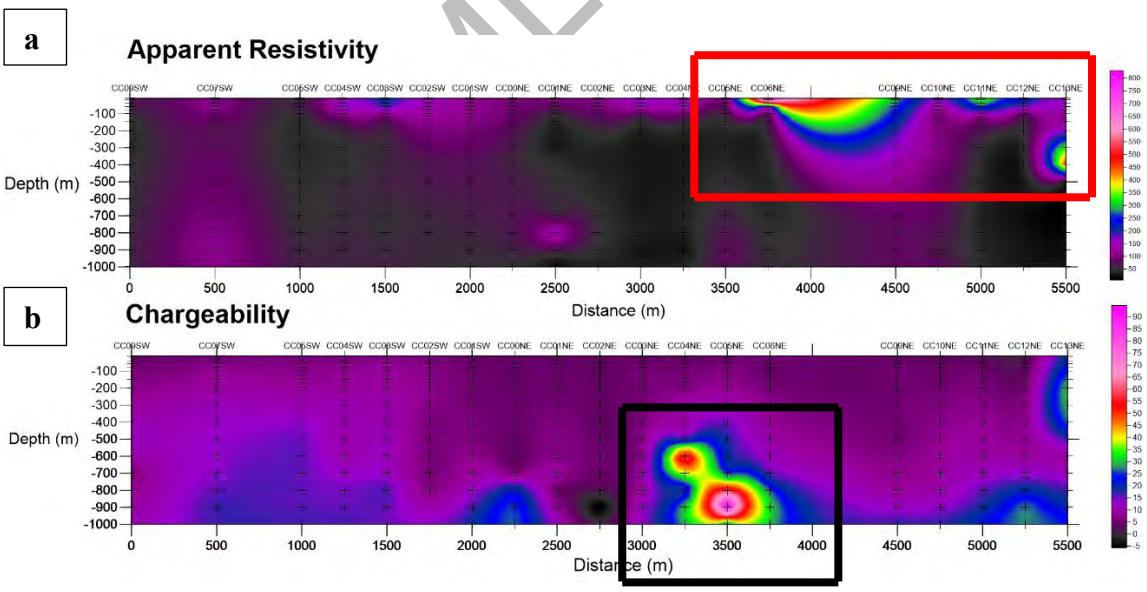

Fig. 5.9: (a) Apparent Resistivity shows increase in values that could not be matched/modeled with master resistivity curves and high resistivity zone is marked with red rectangle. (b) Chargeability Pseudo-sections shows a high chargeability which indicates the probable presence of sulphide mineralization marked in black rectangle.

5.5.4 Interpretation of Profile DD

Some apparent resistivity curves which are deviated from the theoretical master curves are also observed in the vicinity of inferred subsurface concealed fault. The values of the apparent resistivity which are abnormal are not used for the contouring of apparent resistivity pseudo-section (Fig. 5.10).

A continuous increasing trend of IP values are observed with increasing depth. A very good continuous high chargeability zone of about 1500 meter is present in the depth range of 700 to 1000 meters from DD03NE to DD08NE.

These high IP values are most probably corresponded to the presence of sulphide mineralization/graphitic schist.

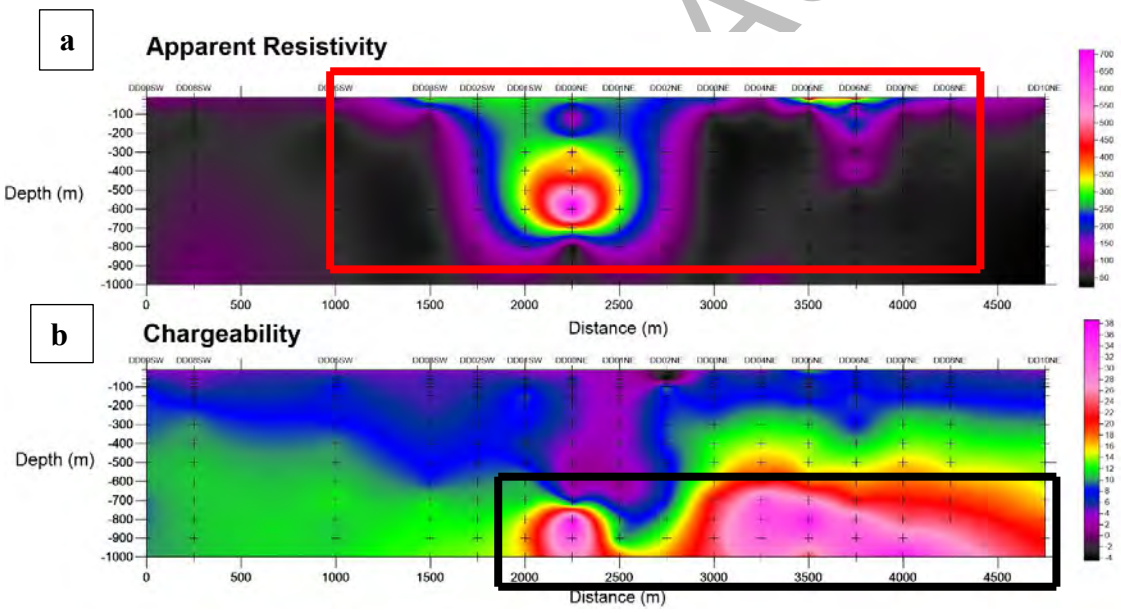

Fig. 5.10: (a) Apparent Resistivity shows deviated behavior from theoretical master curve which is not used for the contouring of apparent resistivity pseudo-section as marked in red rectangle. (b) Chargeability Pseudo-sections shows very high chargeability zone which corresponded to the presence of sulphide mineralization/graphitic schist marked in black rectangle.

7.5.5 Interpretation of Profile EE

The profile orientation is along the Chenab Rivers which is clearly evident by the presence sands with apparent resistivity of 550 ohm-m. The basement depth varies

in the range of 400 to 500 meters. The presence of sand on the surface made it difficult to inject the current and get optimum signals. Therefore, only IP value to the depth of 800 meters could be observed along the profile (Fig.5.11). A good chargeability zone under the depth of 600 meters is observed with lateral extension of about 500 meters on EE00NE and EE02NE observational points.

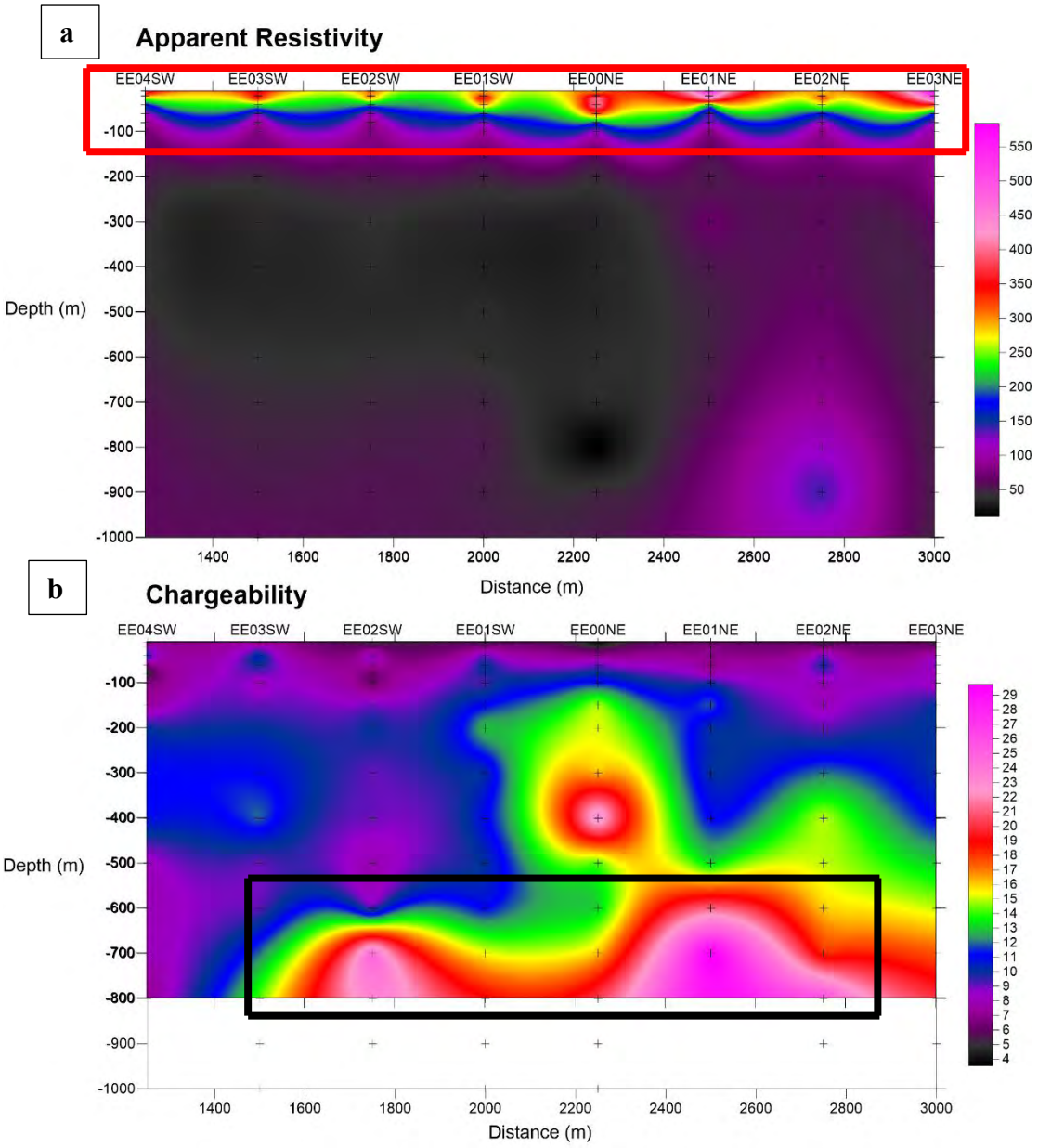

Fig. 5.11: (a) Apparent Resistivity values are not up to mark due to presence of sand on surface & difficult to get optimum signals top surface is marked with red rectangle. (b)Chargeability Pseudo-sections shows good chargeability zone under the depth of 600 meters is observed with lateral extension of about 500 meters marked in black rectangle.

CHAPTER NO. 6

DISCUSSION AND CONCLUSION

6.1 Results and Discussion

The bouguer gravity anomaly map shows the NW-SE trending contours with peak value of 42 mgals. The total magnetic intensity anomaly map of the area also demonstrates the same contours trend with positive peak of magnetic corresponds to the gravity high with very good correlation. The division of magnetic pole into two is probably due to the existence of very close bodies generating the magnetic signal.

It is also evident from the elongation of gravity anomaly at the center of map on western side which is stretched in SE direction. The decrease in gravity is rapid toward NE side of peak anomaly than SW side which leads towards the existence of NW-SE trending fault and the magnetic source (magnetite) probably emplaced along this weak zone. A small positive closure towards the NW corner of the investigated area with peak value of 40 mgals near AA05NE is signal of exposed rocks and at the same time generating the magnetic anomaly of about 400 gammas following the general view that subsurface topography of basement rocks has major contribution towards the gravity effect.

However, the existence of some magnetically susceptible mineral like magnetite, even in disseminated from in host rock will generate the magnetic anomaly of such amplitude, too. And in this area the case seems to be like the same. The contour trend of Bouguer gravity Anomaly Map (Fig.5.3) and Total magnetic Intensity anomaly map (Fig.5.5) are same and anomalous zones of both the maps exist approximately at the same location, confirming the same source generating the signals in both the geophysical methods.

The comparison of residual bouguer gravity and residual total magnetic intensity at an average ring radius of 482 meters (Fig.5.4 & 5.6) show that central magnetic anomalies correspond to the gravity anomalies of about 0.4 mgals. However, the peak gravity anomaly with it central 303788E, 3522709N has no direct relationship with magnetic anomaly. The negative gravity signature on NE direction of gravity peak

in NW-SE direction is the signature of subsurface concealed fault. Another two gravity residual effects of 0.8 and 1.6 mgals respectively are also oriented in NW-SE direction along concealed fault on the NE side. However, no direct correlation is available of those two existed anomalies with magnetic signature.

The chargeability behavior of the area shows existence of high value at the edges of gravity high and comparatively low values over the gravity high. The high chargeability values normally correspond to the sulphide mineralization.

In Wad Sayyidan area the high chargeability zones seem to be present at the contact of basement rocks and metasediments. The resistivity behavior of some of the observed curves near inferred subsurface concealed fault show abnormal behavior and could not be modeled with the master curves.

- The significant values of chargeability at observed profiles are at AA01SW, AA00NE along profile AA (Fig.5.7).

- A zone at depth of about 600 meters from BB00NE to BB03SW along profile BB (Fig.5.8).

- A very high northeast dipping zone on CC04NE and CC05NE along profile CC (Fig.5.9).

- A zone at depth of about 1500 meters from DD03NE to DD08NE along profile DD (Fig.5.10).

- A zone at depth of about 600 meters is observed with lateral extension of about 500 meters on EE00NE and EE02NE along profile EE (Fig.5.11).

- The high chargeability zones along profile CC and DD are at the edge of small gravity anomaly with peak value of 39 mgals in Bouguer gravity anomaly map (Fig. 5.3).

- The depth to basement top varies from 122 to 509 meters along all observed IP/Resistivity profiles. The minimum depth to the top of basement is in the region of high gravity. The top depth of magnetic source as measured by Peter's Half Slope Method for WS-1 is about 220 meters (Fig. 6.1).

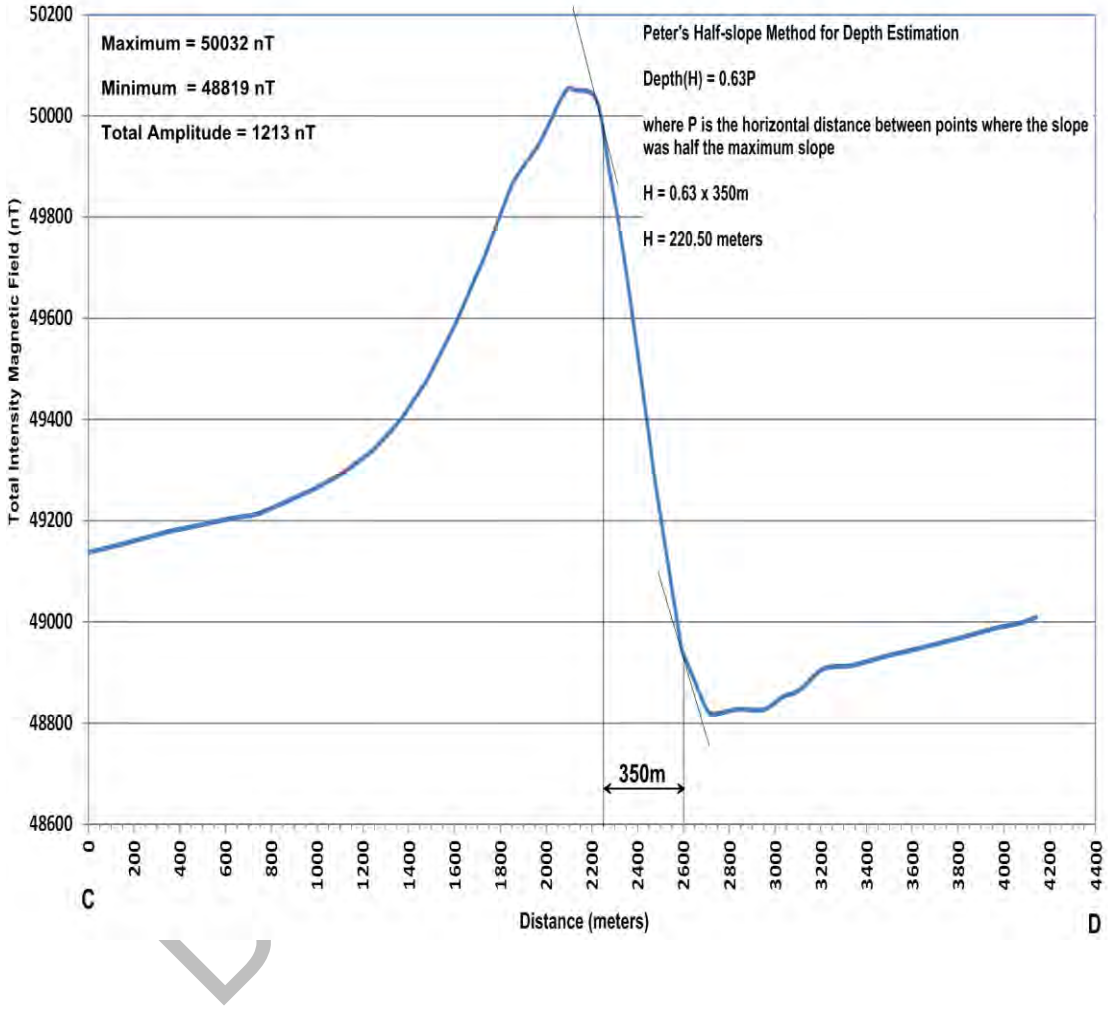

Fig. 6.1: Depth Estimation of Magnetic Source is determined by using Peter's Half Slope Method for drill hole WS-1 as calculated by curve values in above graph is about 220 meters.

6.2 Conclusions

- Total variation of Bouguer gravity in the area is 11 mgals while amplitude of total magnetic intensity is1400 gammas.

- The orientation of gravity and magnetic contours are in NW-SE direction and following the trend observed in semi-detailed magnetic survey.

- Positive bouguer gravity closure is approximately correlated with positive total magnetic intensity pole of main anomaly.

- The small exposed rocks exposure in the area with showings of Specularite producing effect with peak value of 39.5 mgals. Magnetic effect on these rocks is also evident on the total magnetic intensity anomaly map.

- The residual of bouguer gravity and total magnetic intensity show more precise picture of the subsurface geological setup. Two very close bodies producing the effect of magnetic are separated. A subsurface NW-SE trending fault is present just northeast of the peak bouguer gravity.

- The amplitude of residual bouguer gravity at the location of exposed rocks at the position of exposed rocks and the main central anomaly are same, where no exposure is present.

- The depth to the basement in the vicinity of main bouguer gravity peak is about 130 meters. This leads towards the existence of some higher density value of material at the location.

- Three-layer cases are generally observed in the VES in the area with sand at the top after alluvial cover, clays/silt and then basement down to the explored depth.

- The depth to basement at location of bouguer gravity peak is shallower than the flanks on NE and SW direction.

- Some resistivity curves deviate from the theoretical master curves showing irregular subsurface topography of basement shield rocks. This behavior on apparent resistivity curves is observed in the central portion of the mapped area, approximately at the location of inferred fault by bouguer gravity signature.

- Large variation in chargeability is observed with higher values just outside the positive bouguer gravity closure and possibility of sulphide mineralization is there at the contact of volcanic rocks and metasediments.

- Promising zones for sulphide mineralization occurrence is there along profile CC with high chargeability and corresponding low resistivities.

- The correlation of positive bouguer gravity and magnetic may leads to the occurrence of magnetically susceptible minerals in the vicinity.

After interpretation of integrated geophysical methods (Gravity, Magnetic and IP/Resistivity data) following test drill holes are proposed. But drilling at only one location (WS-1) was carried out. The outcome of the drill hole WS-1 was not communicated (Table 6.1).

Table. 6.1: Proposed Drill Hole Locations after Interpretation

Drill Hole No.	Location
WS-1	304720E 3522433N
WS-2	303798E 3522690N
WS-3	305677E 3523015N

REFERENCES

Abraham, E.M. and Alile, O.M., 2019. Modelling subsurface geologic structures at the Ikogosi geothermal field, southwestern Nigeria, using gravity, magnetics and seismic interferometry techniques. *Journal of Geophysics and Engineering*, *16*(4), pp.729-741.

Adams, A.E., MacKenzie, W.S. and Guilford, C., 2017. *Atlas of sedimentary rocks under the microscope*. Routledge.

Adel, S., Ardeshir, H. and Aref, S., 2022. Geophysical explorations by resistivity and induced polarization methods for the copper deposit, South Khorasan, Iran. *Известия Томского политехнического университета. Инжиниринг георесурсов*, *333*(3), pp.99

Akhtar, M. et. al., 1998 Preliminary report on Iron Mineralization in Churnali area, Sargodha District, Punjab, Pakistan., I.R. No. 658, G.S.P., Quetta.

Akhtar, M. et. al., 1998. Urban Geology and Environment Concerns of Sargodha area, Sargodha District, Punjab, Pakistan., I.R. No.655, G.S.P., Quetta.

Alam, G.S. et al., 1993 Aggregate resources of Kirana Hills, District Sargodha, Punjab, Pakistan, GSP, IR.381.

Alam, G.S. et al.,1990 Discovery of Iron Ore Deposits in the Buried Pre-Cambrian Shield Rocks of Punjab Plains, Chiniot Area, Jhang District, Punjab, Pakistan., I.R.No.427, G.S.P., Quetta.

Butt, M.H. et. al.1993 Integrated Geophysical Investigations for Iron Ore in Chiniot area, Punjab, Pakistan., Record Vol. 101., G.S.P., Quetta.

Chaudhry, M. N., Ahmad, S. A., & Mateen, A. (1999). Some postulates on the tectonomagmatism, tectonostratigraphy and economic potential of Kirana-Malani-Basin, IndoPakistan. *Pakistan Journal of Hydrocarbon Research, 11*, 52-68.

Chaudhry, M.N., Ahsan, N. and Rehman, S.U., 2022. Revised stratigraphy of Sargodha-Chiniot Area Punjab, Pakistan. *Geol. Bull. Punjab Univ*, *46.*

Dahlin, T., Leroux, V. and Nissen, J., 2002. Measuring techniques in induced polarisation imaging. *Journal of Applied Geophysics*, *50*(3), pp.279-298.

Davies, R.G. and Crawford, A.R., 1971. Petrography and age of the rocks of Bulland

hill, Kirana hills, Sarghoda District, Pakistan. *Geological Magazine*, *108*(3), pp.235

Davis, R.G..et.al. 1971 Petrography and age of the rocks of Bulland Hill, Kirana Hills, Sargodha District, West Pakistan.Geol.Mag.,108:235-246.

Dentith, M., Mudge, S.T.- 2014. Geophysics for the mineral exploration geoscientist. Cambridge University Press, 454p.

Dobrin, M.B., 1981 Introduction to Geophysical Prospecting (3rd edition), McGraw-Hill Book Company.

Ervin, C.P., 1977. Theory of the Bouguer anomaly. *Geophysics*, *42*(7), p.1468.

Farah, A. et. Al 1964 Gravity Base Stations in W. Pakistan, Vol. XI, Part2.GSP Quetta

Gay, S.P., 1963. Standard curves for interpretation of magnetic anomalies over long tabular bodies. *Geophysics*, *28*(2), pp.161-200.

Gearhart, R.L., 2013. Magnetometer Survey and Testing. *Maritime Archaeology: A Reader of Substantive and Theoretical Contributions*, p.291.

Gee, E.R. and Gee, D.G., 1989. Overview of the geology and structure of the Salt Range, with observations on related areas of northern Pakistan. *Geological Society of America special paper*, *232*, pp.95-112.

Gupta, P.K., Niwas, S. and Gaur, V.K., 1997. Straightforward inversion of vertical electrical sounding data. *Geophysics*, *62*(3), pp.775-785.

Haider, N., Khan, S., Siddiqui, R.H. and Iqbal, S., 2021. Genesis of Langrial Iron Ore of Hazara area, Khyber Pakhtunkhwa, Pakistan. *Journal of Geography and Cartography*, *4*(2), pp.82-89.

Herman, R., 2001. An introduction to electrical resistivity in geophysics. *American Journal of Physics*, *69*(9), pp.943-952.

Hinze, W.J., Von Frese, R.R., Von Frese, R. and Saad, A.H., 2013. *Gravity and magnetic exploration: Principles, practices, and applications*. Cambridge University.

Javaid, S., 2002 Computer Applications in the Evaluation of 2nd-Derivative and Residual of Potential Field Data., I.R. No. 769, G.S.P., Quetta.

Jeng, Y., Lee, Y.L., Chen, C.Y. and Lin, M.J., 2003. Integrated signal enhancements in magnetic investigation in archaeology. *Journal of Applied Geophysics*, *53*(1),pp.31-48.

Kazmi and Jan1997. Geology and tectonics of Pakistan. Geographic Publishers, Karachi, Pakistan.

Kearey, P., Brooks, M. and Hill, I., 2002. *An introduction to geophysical exploration* (Vol. 4). John Wiley & Sons.

Khan, Z.K., Ahsan, N., Mateen, A., and Chaudhry, M. N., 2009. Petrography and mineralogy of dolerites of Hachi Volcanics, Kirana hills area, Pakistan. *Geol. Bull. Punjab Univ*, *44*, pp.55-67.

LaFehr, T.R., 1991. Standardization in gravity reduction. *Geophysics*, *56*(8), pp.1170

Lenz, J.E., 1990. A review of magnetic sensors. *Proceedings of the IEEE*, *78*(6), pp.973

Malkani, M.S. and Mahmood, Z., 2016. Revised stratigraphy of Pakistan. *Geological Survey of Pakistan, Record*, *127*, pp.1-87.

Naeem, M., Zafar, T., Touseef Bilal, M. and Oyebamiji, A., 2019. Physical characterization and alkali carbonate reactivity (ACR) potential of the rocks from Bauhti Pind and Bajar area Hassan Abdal, Pakistan. *SN Applied Sciences*, *1*, pp.1-9.

Odera, P.A. and Jatani, A.I., 2017. Assessment of Hand-held GPS Surveying in Land Adjudication: A Case Study of Ngoliba Settlement Scheme in Kenya. *Journal of Agriculture, Science and Technology*, *18*(1), pp.24-37.

Parasnis, D.S., 2012. *Principles of applied geophysics*. Springer Science & Business M

Parker,E.N.,1970.The origin of magnetic fields. *The Astrophysical Journal*, *160*, p.383.

Powell, C. McA., 1979. A Speculative tectonic history of Pakistan and surroundings: Some constraints from the Indian Ocean. In: Farah, A. & Dejong, K.A. (eds) Geodynamics of Pakistan. Geol. Survey. Pak., Quetta,5-24.

Telford, W.M. et al. 1976. Applied Geophysics (1st edition), Cambridge University Press, London.

ZharikovF, V.A., 2007. 9. Metasomatism and metasomatic rocksF. *A classification of metamorphic rocks and glossary of terms. Recommendations of the International Union of Geological Sciences Subcommission on the Systaematics of Metamorphic Rocks*.

Zohdy. A. A. R. et. al.1980 Techniques of Water-Resources Investigations of the United States Geological Survey (2nd edition). United States Government Printing Office,WDC.

Appendix

Wad Sayyidan
Vertical Electrical Soundings
Modeled Resistivity Curves

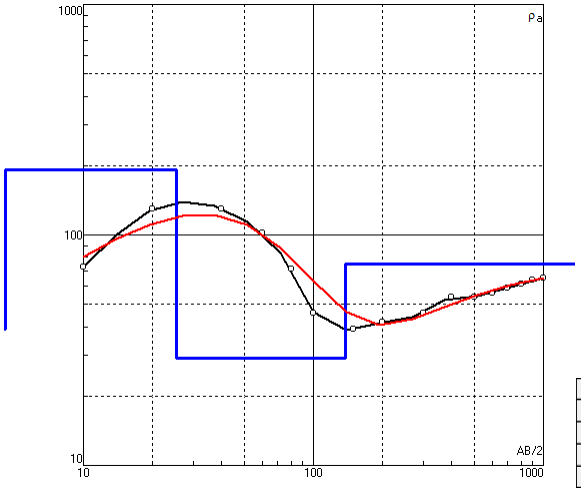

AA00NE

N	1	2	3	4
ρ	39.2	192	29.2	74.8
h	3.24	22.1	112	
d	3.24	25.3	137	
Alt	-3.24	-25.34	-137.3	

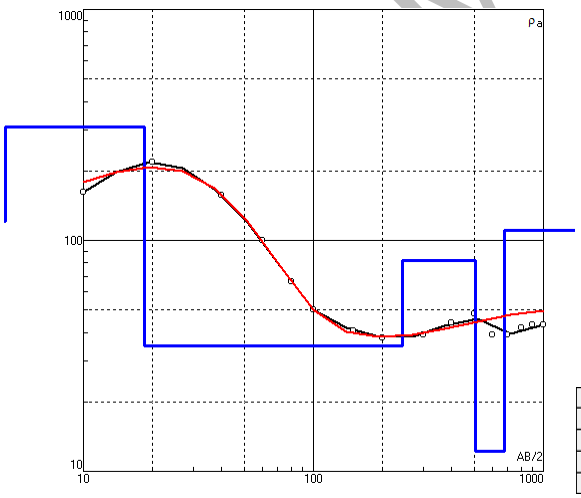

AA04NE

N	1	2	3	4	5	6
ρ	121	310	34.9	82.2	12.2	111
h	3.85	14.6	226	261	170	
d	3.85	18.5	244	505	675	
Alt	-3.85	-18.45	-244.4	-505.5	-675.5	

AA05NE

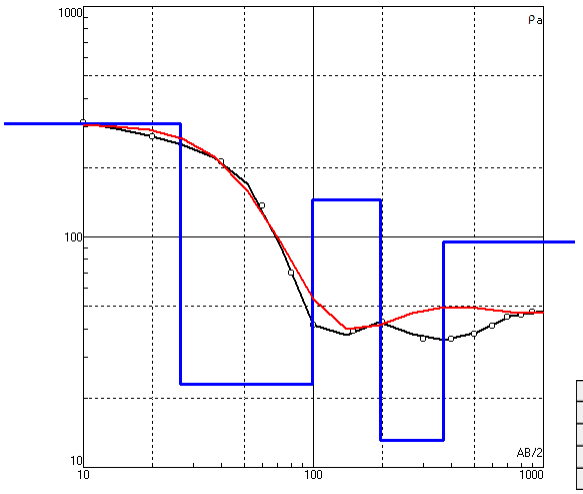

N	1	2	3	4	5
ρ	310	23	145	13.1	95.1
h	26.5	72.5	96.6	172	
d	26.5	99	196	368	
Alt	-26.5	-99	-195.6	-367.6	

AA01SW

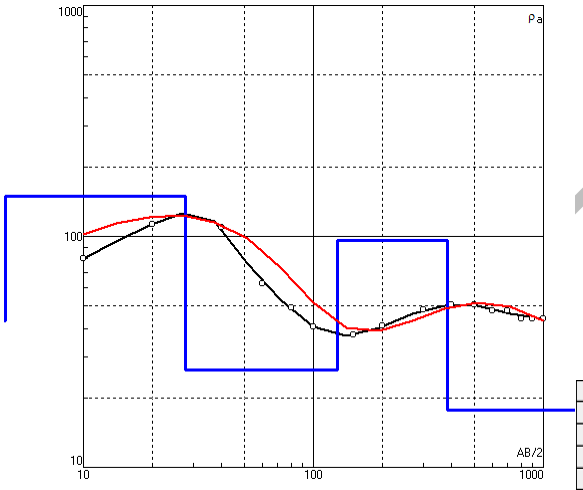

N	1	2	3	4	5
ρ	43.3	149	26.4	96.1	17.7
h	1.83	25.9	99.4	254	
d	1.83	27.7	127	381	
Alt	-1.83	-27.73	-127.1	-381.1	

AA02SW

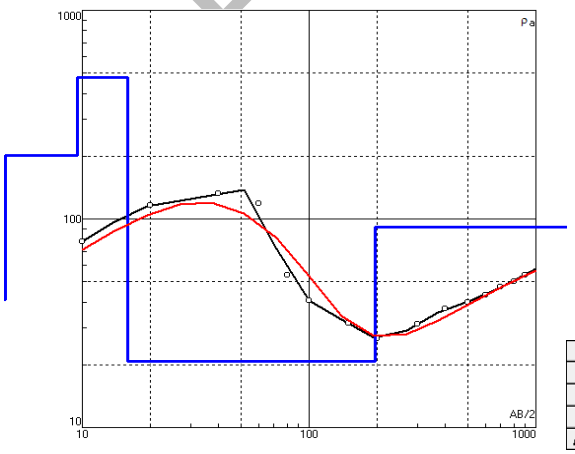

N	1	2	3	4	5
ρ	41	202	476	20.8	91.4
h	4.35	5.13	6.37	180	
d	4.35	9.48	15.8	196	
Alt	-4.35	-9.48	-15.85	-195.9	

BB00NE

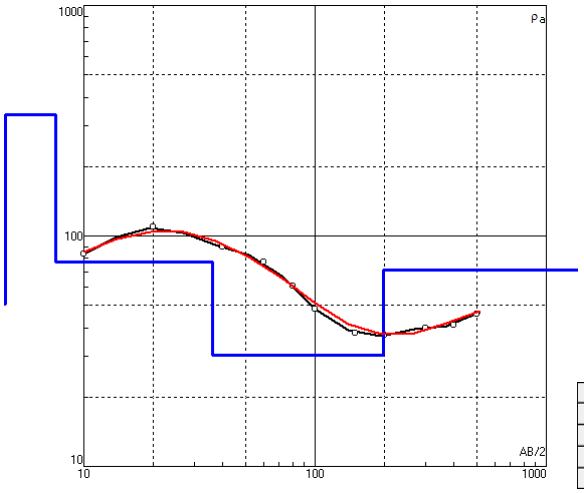

N	1	2	3	4	5
ρ	50.8	335	77	30.4	71.2
h	4.07	3.46	28.5	162	
d	4.07	7.53	36	198	
Alt	-4.07	-7.53	-36.03	-198	

BB03NE

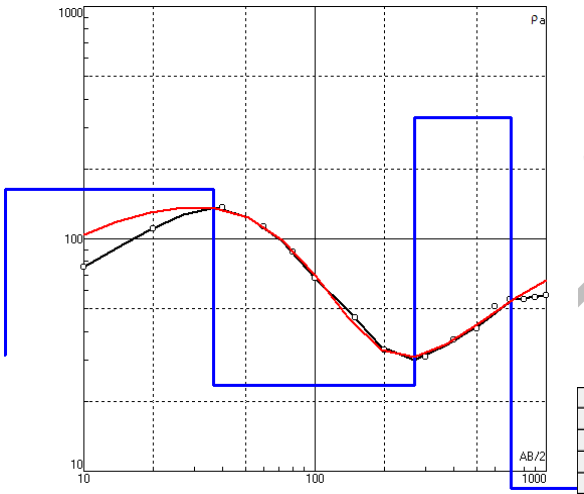

N	1	2	3	4	5
ρ	31.7	163	23.4	334	7.03
h	1.41	34.8	234	435	
d	1.41	36.2	270	705	
Alt	-1.41	-36.21	-270.2	-705.2	

BB04NE

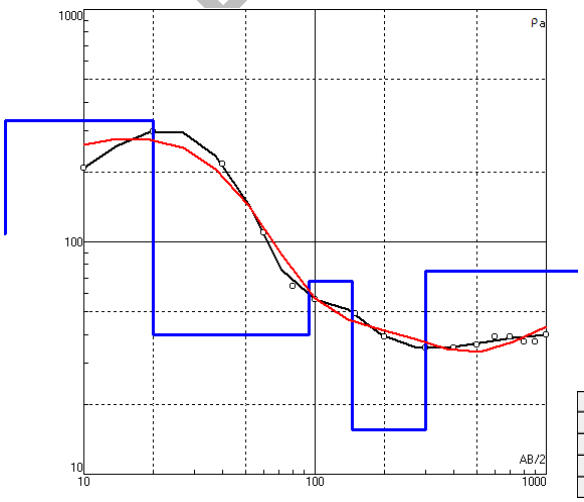

N	1	2	3	4	5	6
ρ	108	334	39.8	67.6	15.5	74.8
h	1.33	18.6	74.2	50.7	157	
d	1.33	19.9	94.1	145	302	
Alt	-1.33	-19.93	-94.13	-144.8	-301.8	

BB07NE

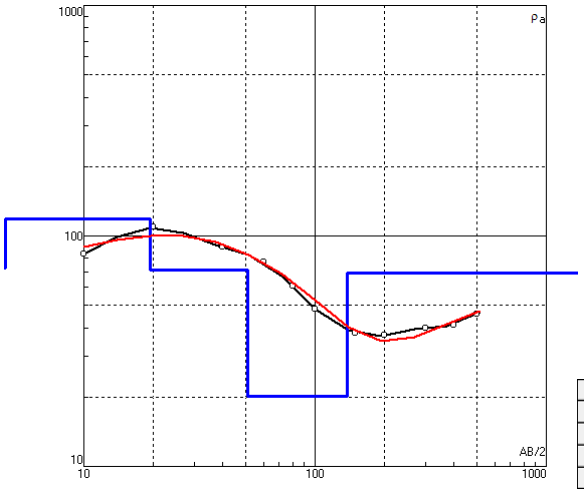

N	1	2	3	4	5
ρ	72.6	119	71.1	20.1	69
h	4.06	15.3	31.9	86.4	
d	4.06	19.4	51.3	138	
Alt	-4.06	-19.36	-51.26	-137.7	

BB01SW

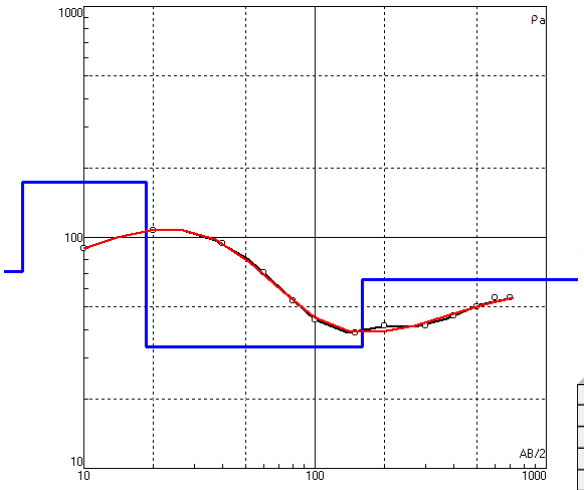

N	1	2	3	4
ρ	71.23	174.2	33.43	65.86
h	5.451	13.15	140.9	
d	5.451	18.6	159.5	
Alt	-5.451	-18.601	-159.5	

BB02SW

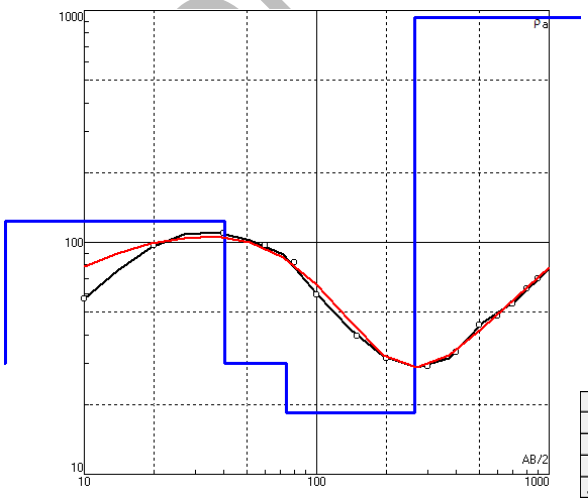

N	1	2	3	4	5
ρ	30.2	124	30.1	18.4	932
h	1.83	38.2	33.7	190	
d	1.83	40	73.7	264	
Alt	-1.83	-40.03	-73.73	-263.7	

BB03SW

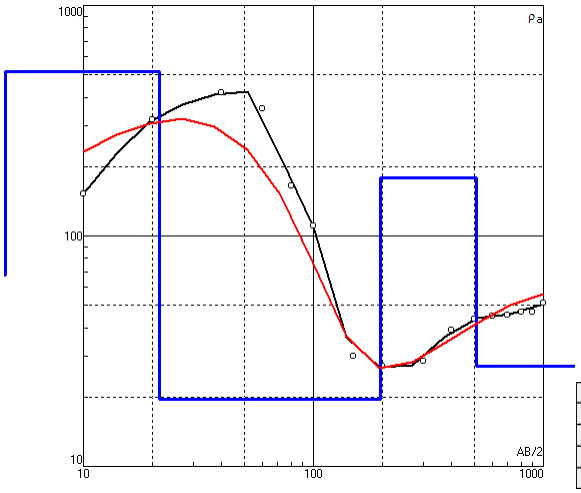

N	1	2	3	4	5
ρ	67.8	516	19.5	178	27.1
h	1.78	19.7	175	316	
d	1.78	21.5	196	512	
Alt	-1.78	-21.48	-196.5	-512.5	

CC00NE

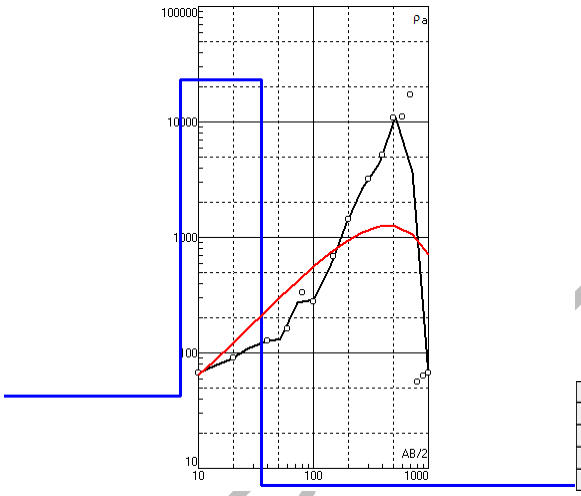

N	1	2	3
ρ	42.2	23413	3.35
h	6.92	28.1	
d	6.92	35	
Alt	-6.92	-35.02	

CC01NE

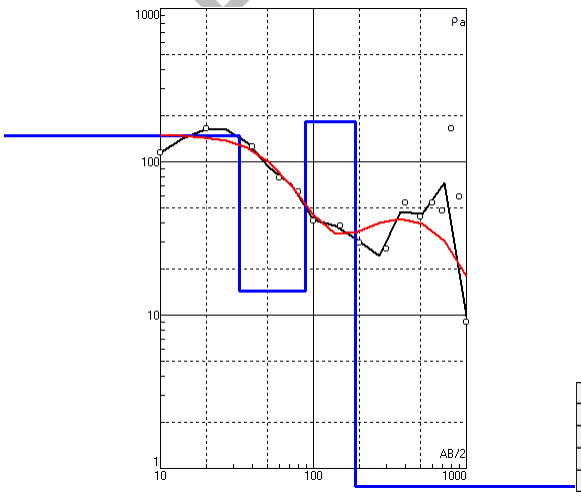

N	1	2	3	4
ρ	149	14.4	183	0.285
h	32.6	56.7	98.6	
d	32.6	89.3	188	
Alt	-32.6	-89.3	-187.9	

CC02NE

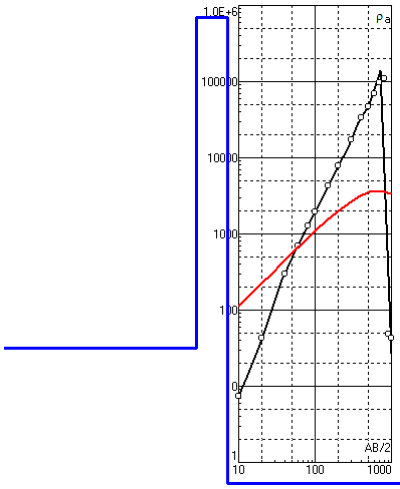

N	1	2	3							
ρ	31.8	7.0E+5	0.371							
h	2.81	4.4								
d	2.81	7.21								
Alt	-2.81	-7.21								

CC03NE

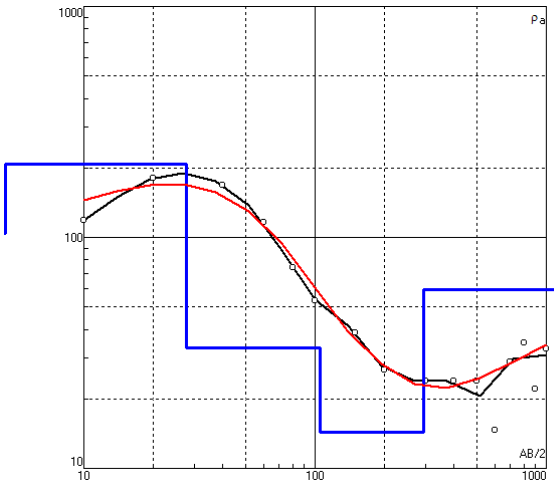

N	1	2	3	4	5					
ρ	104	208	33.4	14.4	59.5					
h	3.57	24.3	77.4	191						
d	3.57	27.9	105	296						
Alt	-3.57	-27.87	-105.3	-296.3						

CC04NE

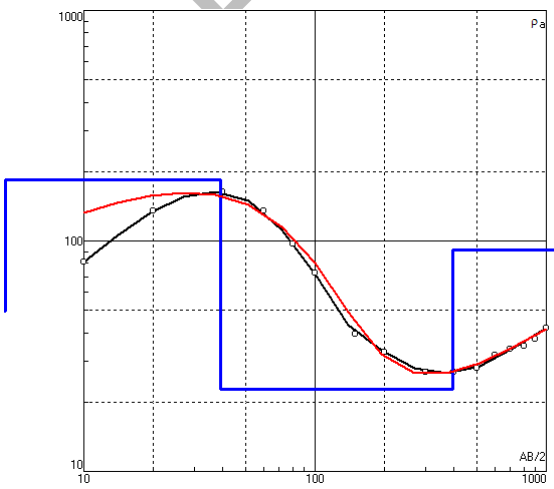

N	1	2	3	4						
ρ	49.4	184	22.7	91.7						
h	1.5	37.7	353							
d	1.5	39.2	392							
Alt	-1.5	-39.2	-392.2							

CC05NE

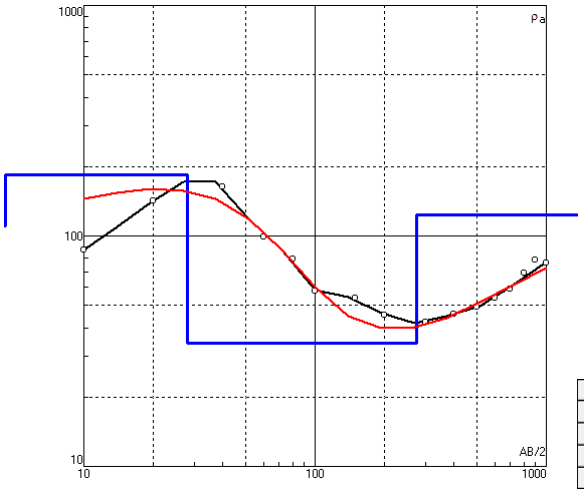

N	1	2	3	4							
ρ	111	185	34.3	123							
h	3.43	24.6	246								
d	3.43	28	274								
Alt	-3.43	-28.03	-274								

CC06NE

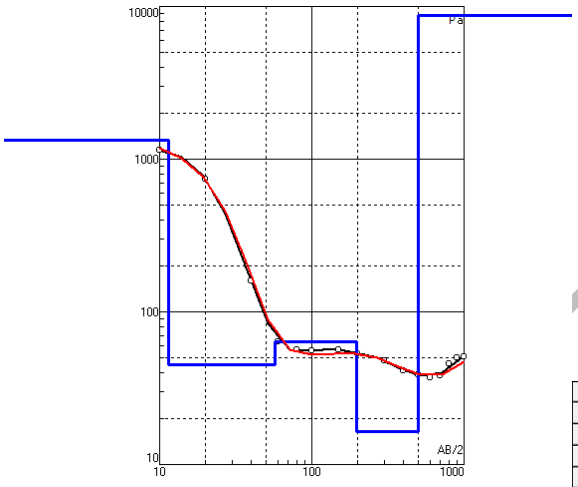

N	1	2	3	4	5						
ρ	1324	45	64.1	16.4	8734						
h	11.4	45.9	140	304							
d	11.4	57.3	197	501							
Alt	-11.4	-57.3	-197.3	-501.3							

CC09NE

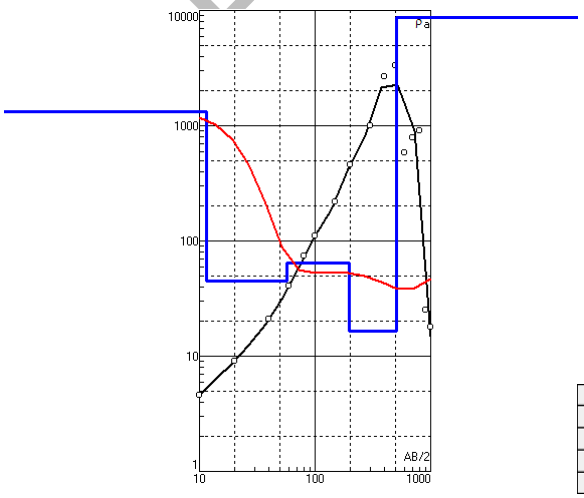

N	1	2	3	4	5						
ρ	1324	45	64.1	16.4	8734						
h	11.4	45.9	140	304							
d	11.4	57.3	197	501							
Alt	-11.4	-57.3	-197.3	-501.3							

CC10NE

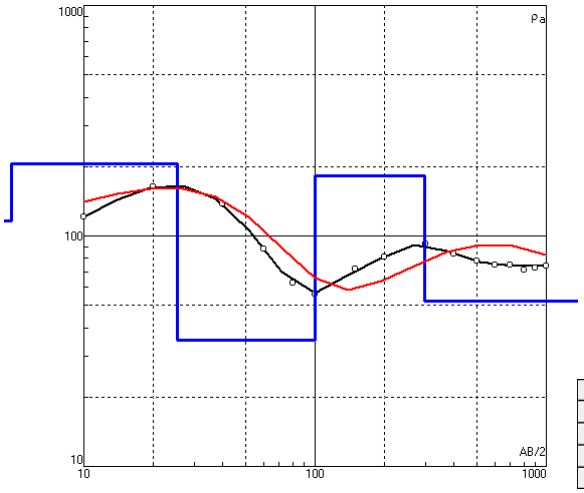

N	1	2	3	4	5						
ρ	116	206	35.4	182	52						
h	4.87	20.5	74.6	197							
d	4.87	25.4	100	297							
Alt	-4.87	-25.37	-99.97	-297							

CC11NE

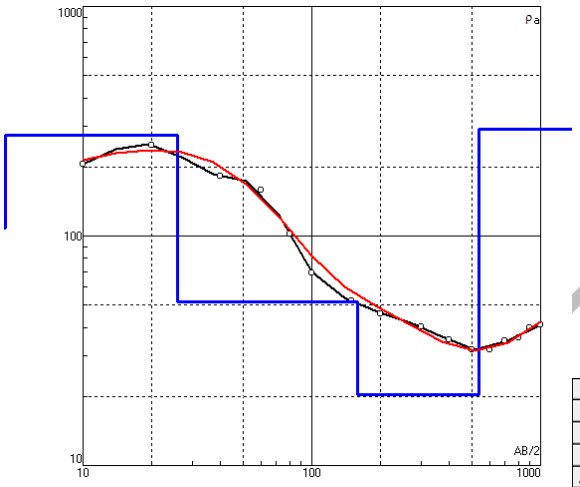

N	1	2	3	4	5						
ρ	108	274	51.6	20.4	292						
h	1.78	24	133	381							
d	1.78	25.8	159	540							
Alt	-1.78	-25.78	-158.8	-539.8							

CC12NE

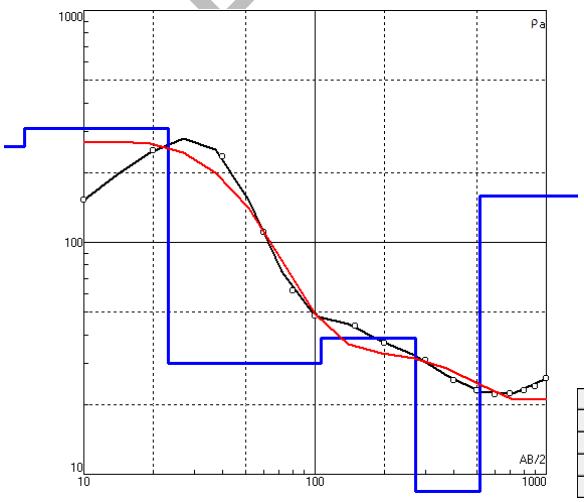

N	1	2	3	4	5	6					
ρ	259	310	30.1	38.6	6.12	158					
h	5.54	17.6	83	166	245						
d	5.54	23.1	106	272	517						
Alt	-5.54	-23.14	-106.1	-272.1	-517.1						

CC13NE

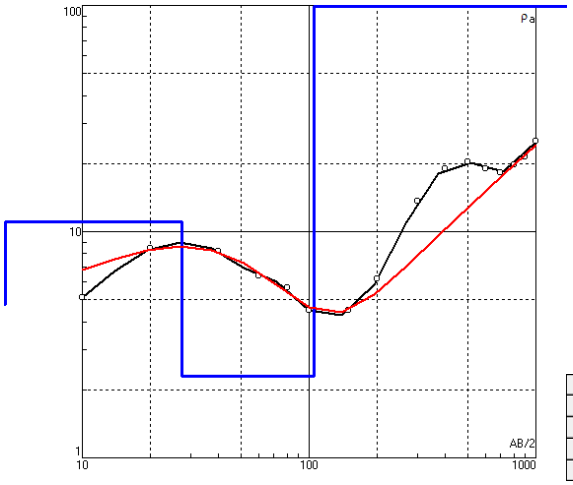

N	1	2	3	4
ρ	4.77	11.1	2.29	195
h	4.07	23.4	77.8	
d	4.07	27.5	105	
Alt	-4.07	-27.47	-105.3	

CC01SW

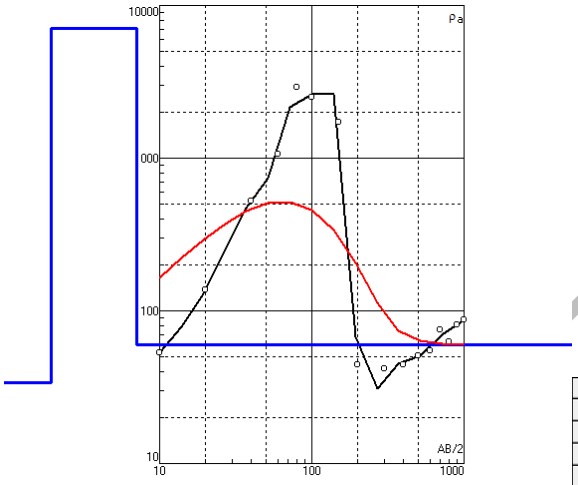

N	1	2	3
ρ	34	7085	59.6
h	1.95	5.09	
d	1.95	7.04	
Alt	-1.95	-7.04	

CC02SW

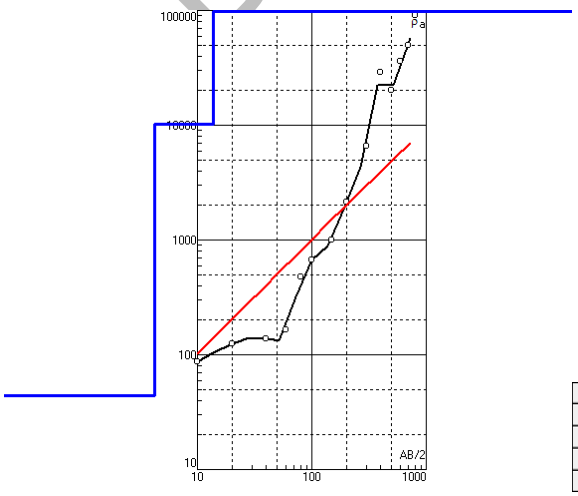

N	1	2	3
ρ	43.7	10271	1.6E+5
h	4.26	9.64	
d	4.26	13.9	
Alt	-4.26	-13.9	

CC03SW

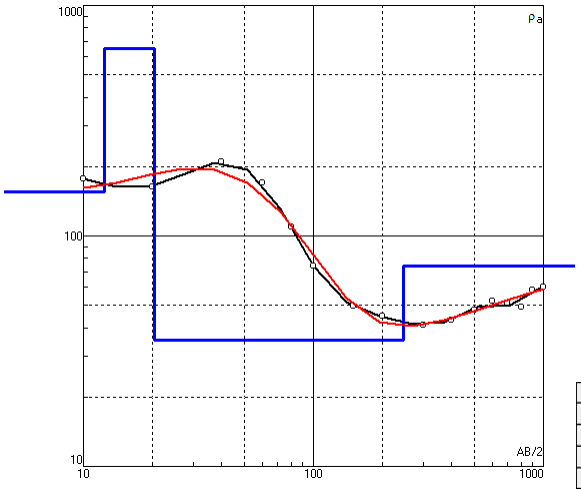

N	1	2	3	4							
ρ	155	653	35.4	74.4							
h	12.3	8.01	227								
d	12.3	20.3	247								
Alt	-12.3	-20.31	-247.3								

CC04SW

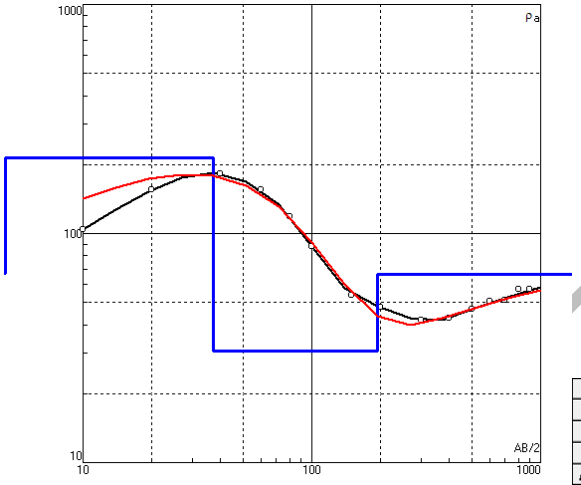

N	1	2	3	4							
ρ	67.3	213	30.7	66.3							
h	2.21	34.9	157								
d	2.21	37.1	194								
Alt	-2.21	-37.11	-194.1								

CC05SW

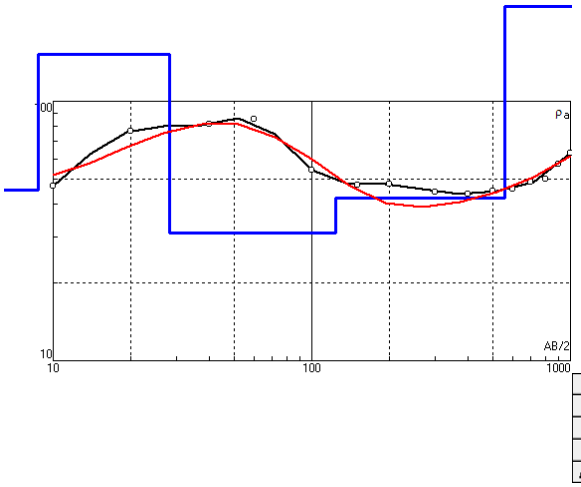

N	1	2	3	4	5						
ρ	45.5	152	31.1	42.4	232						
h	8.77	19.4	95.7	435							
d	8.77	28.2	124	559							
Alt	-8.77	-28.17	-123.9	-558.9							

CC07S

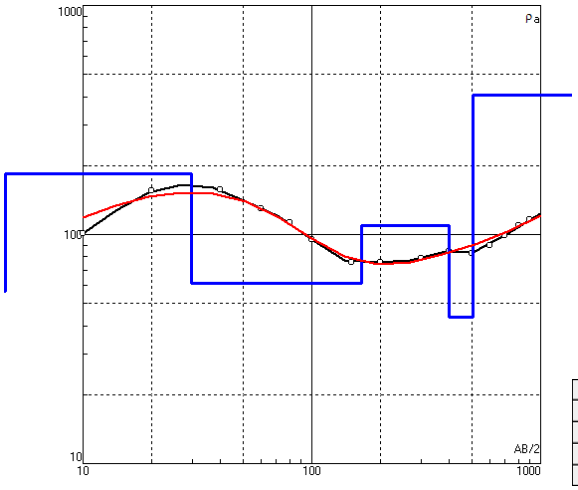

N	1	2	3	4	5	6
ρ	56.3	184	61.5	109	43.7	406
h	2.27	27.5	135	235	105	
d	2.27	29.8	165	400	505	
Alt	-2.27	-29.77	-164.8	-399.8	-504.8	

CC09SW

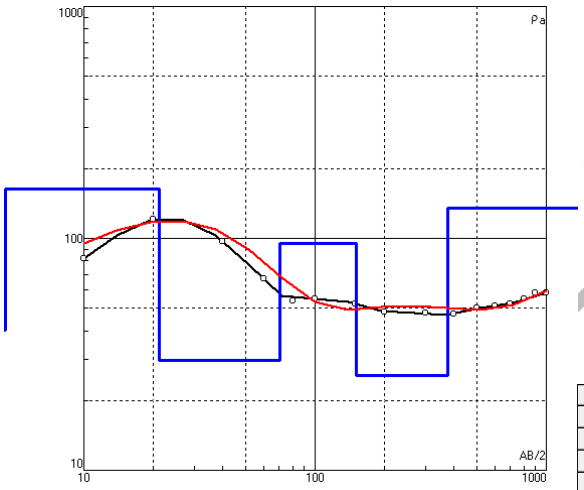

N	1	2	3	4	5	6
ρ	40.1	164	29.9	95	25.6	135
h	2.16	19	49.4	79.6	225	
d	2.16	21.2	70.6	150	375	
Alt	-2.16	-21.16	-70.56	-150.2	-375.2	

DD00NE

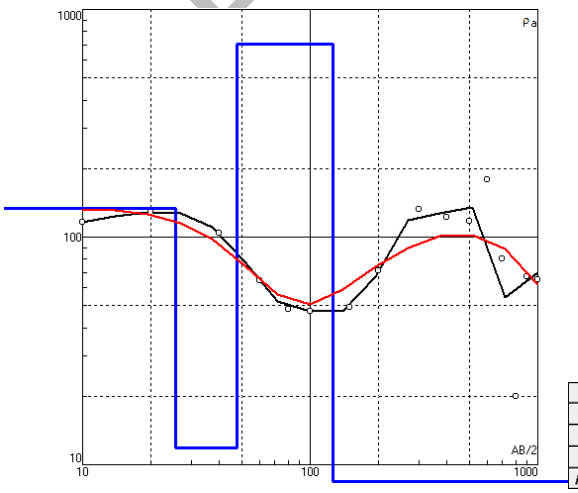

N	1	2	3	4
ρ	134	11.9	705	1.17
h	25.6	22.2	78	
d	25.6	47.8	126	
Alt	-25.6	-47.8	-125.8	

DD01NE

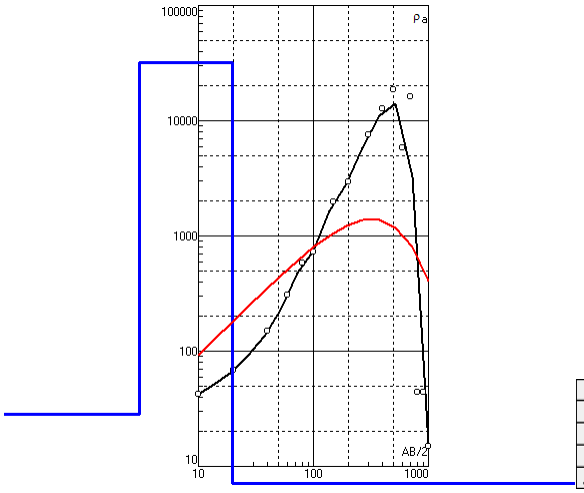

N	1	2	3
ρ	28.1	31702	2.11
h	3.06	16.8	
d	3.06	19.9	
Alt	-3.06	-19.86	

DD02NE

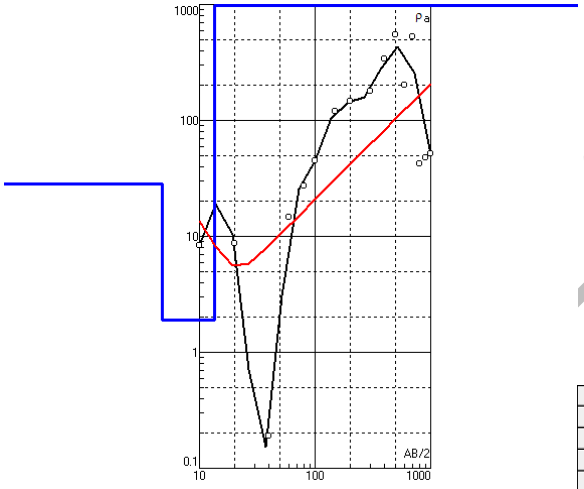

N	1	2	3
ρ	28.3	1.89	11532
h	4.81	8.7	
d	4.81	13.5	
Alt	-4.81	-13.51	

DD03NE

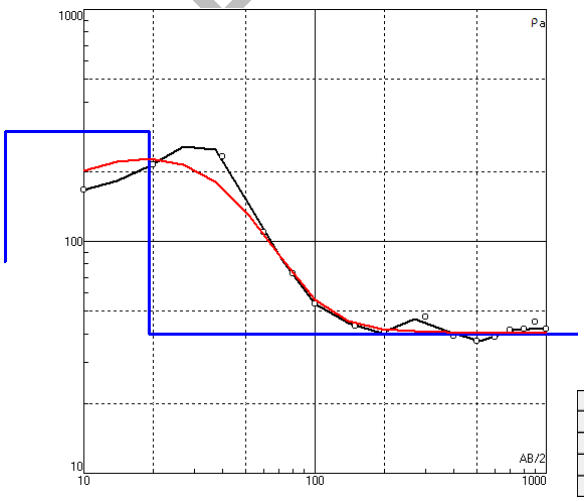

N	1	2	3
ρ	82	297	40
h	1.7	17.4	
d	1.7	19.1	
Alt	-1.7	-19.1	

DD04NE

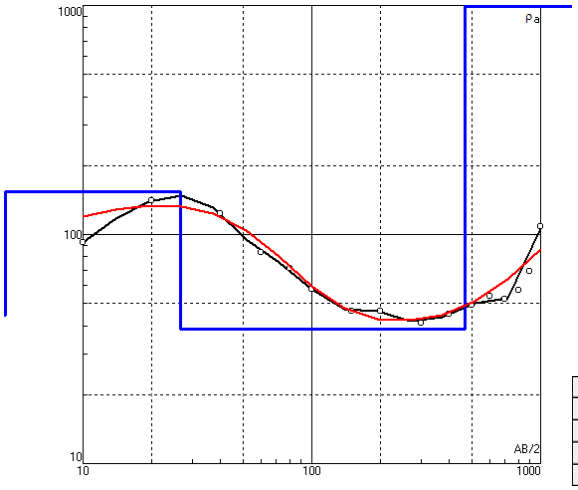

N	1	2	3	4						
ρ	44.3	154	38.6	8271						
h	1.27	25.4	441							
d	1.27	26.7	468							
Alt	-1.27	-26.67	-467.7							

DD05NE

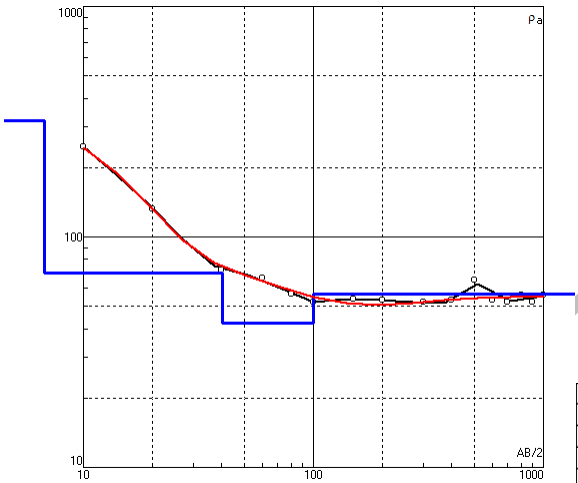

N	1	2	3	4						
ρ	320	69.8	42.1	56.3						
h	6.8	33.3	59.9							
d	6.8	40.1	100							
Alt	-6.8	-40.1	-100							

DD06NE

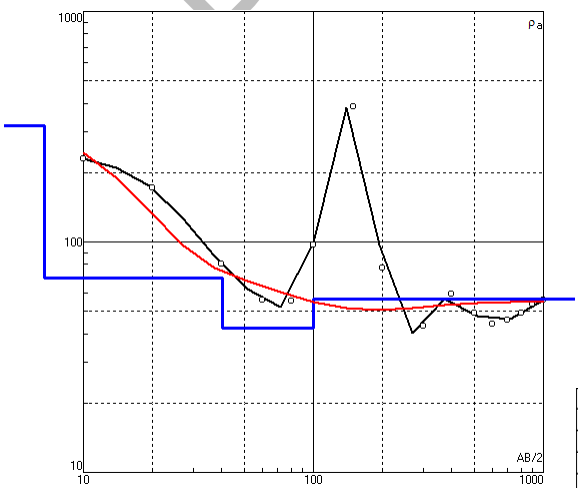

N	1	2	3	4						
ρ	320	69.8	42.1	56.3						
h	6.8	33.3	59.9							
d	6.8	40.1	100							
Alt	-6.8	-40.1	-100							

DD07NE

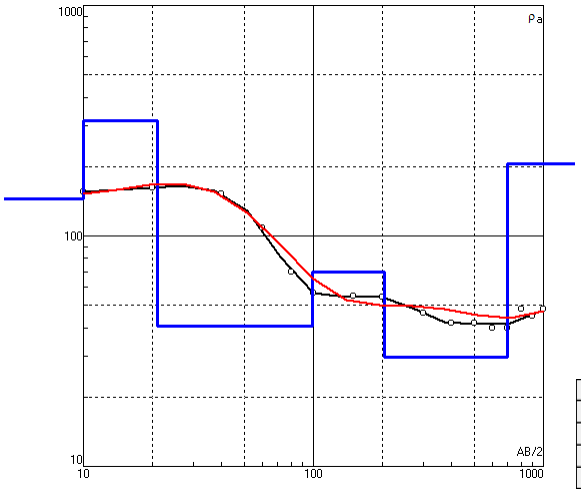

N	1	2	3	4	5	6
ρ	145	315	40.6	69.5	29.7	205
h	9.98	10.9	77.7	105	497	
d	9.98	20.9	98.6	204	701	
Alt	-9.98	-20.88	-98.58	-203.6	-700.6	

DD08NE

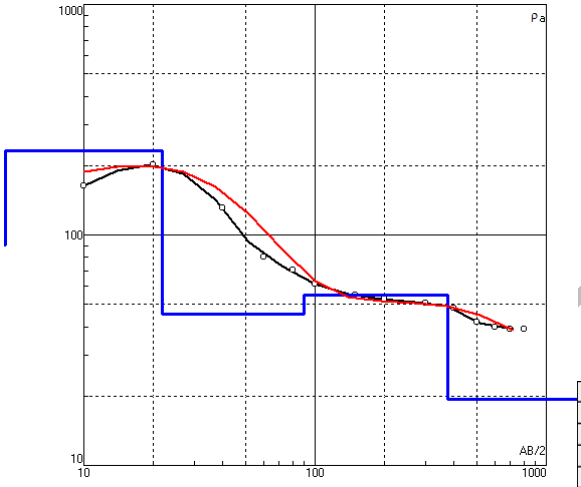

N	1	2	3	4	5
ρ	90.1	231	45.3	55.1	19.4
h	1.47	20.3	67.9	285	
d	1.47	21.8	89.7	375	
Alt	-1.47	-21.77	-89.67	-374.7	

DD10NE

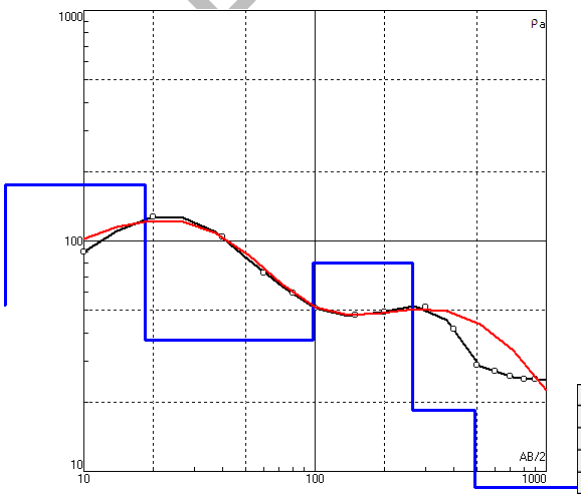

N	1	2	3	4	5	6
ρ	52.9	176	37	80.4	18.4	8.52
h	2.74	15.7	79.4	165	228	
d	2.74	18.4	97.8	263	491	
Alt	-2.74	-18.44	-97.84	-262.8	-490.8	

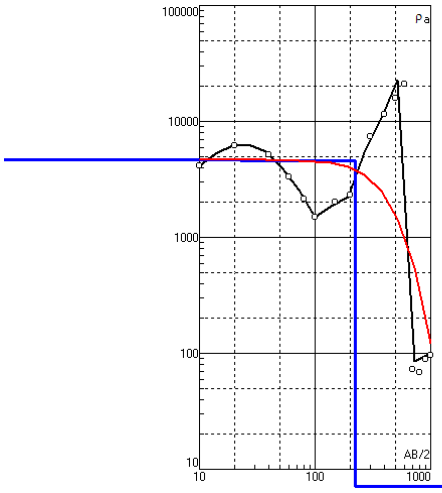

DD01SW

N	1	2	3							
ρ	4674	4562	2.3							
h	22.5	199								
d	22.5	222								
Alt	-22.5	-221.5								

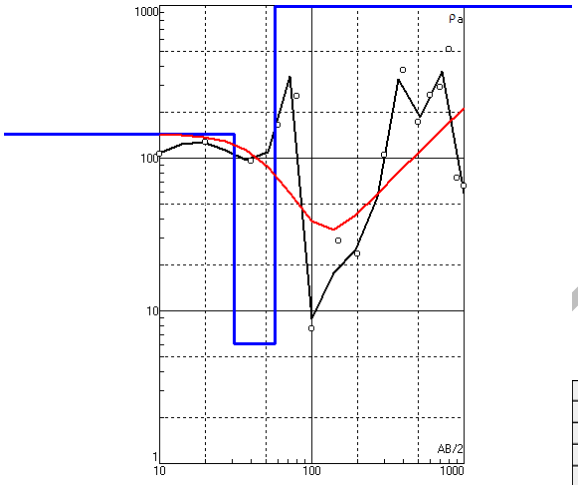

DD02SW

N	1	2	3							
ρ	143	6.1	7830							
h	31.1	26.5								
d	31.1	57.6								
Alt	-31.1	-57.6								

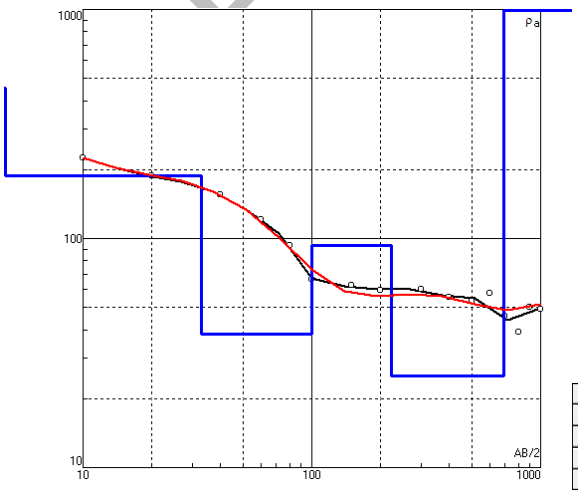

DD03SW

N	1	2	3	4	5	6					
ρ	454	188	38.1	93.7	25.2	2881					
h	2.35	30.6	67.1	122	468						
d	2.35	33	100	222	690						
Alt	-2.35	-32.95	-100.1	-222.1	-690						

DD05S

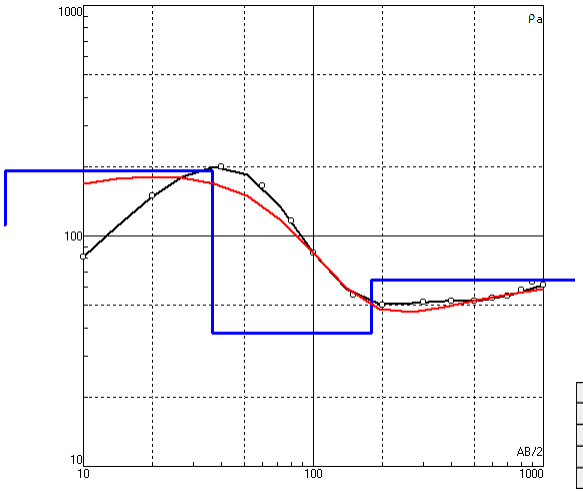

N	1	2	3	4
ρ	112	192	37.8	64.2
h	1.89	34.5	142	
d	1.89	36.4	178	
Alt	-1.89	-36.39	-178.4	

DD08S

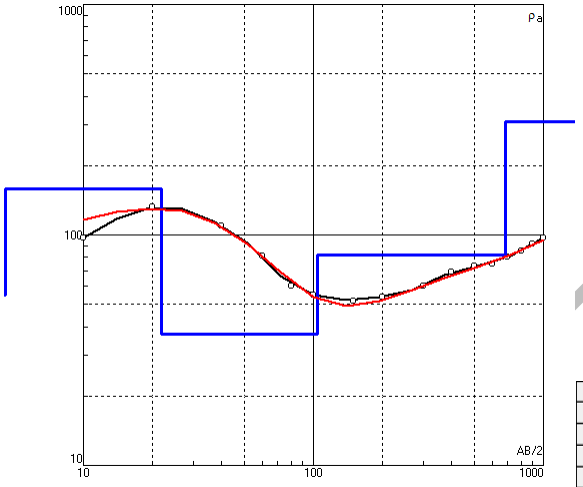

N	1	2	3	4	5
ρ	55.1	158	37.2	82.2	311
h	1.87	20	81.8	577	
d	1.87	21.9	104	681	
Alt	-1.87	-21.87	-103.7	-680.7	

DD09SW

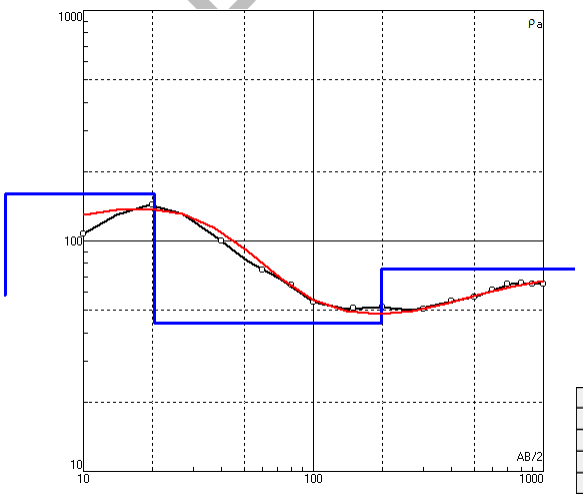

N	1	2	3	4
ρ	58.5	160	44	75.5
h	1.39	19	178	
d	1.39	20.4	198	
Alt	-1.39	-20.39	-198.4	

EE00NE

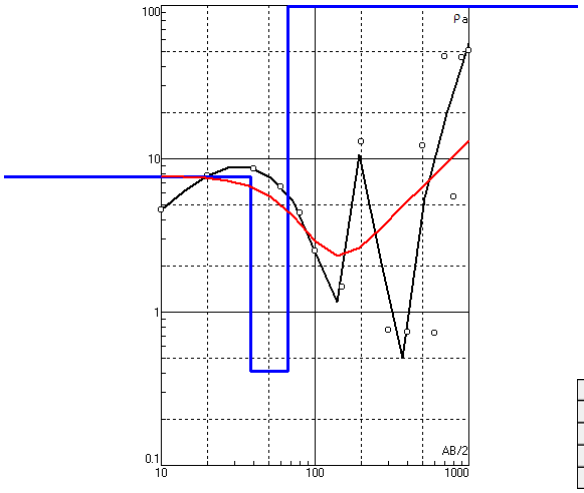

N	1	2	3							
ρ	7.64	0.411	1864							
h	37.9	29.1								
d	37.9	67								
Alt	-37.9	-67								

EE01NE

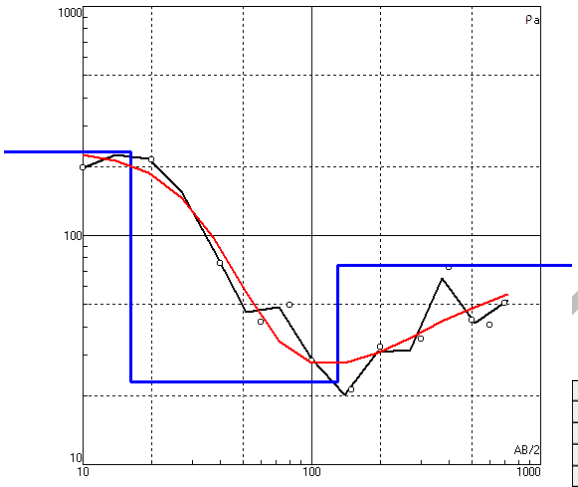

N	1	2	3							
ρ	233	23	74.2							
h	16.1	114								
d	16.1	130								
Alt	-16.1	-130.1								

EE02NE

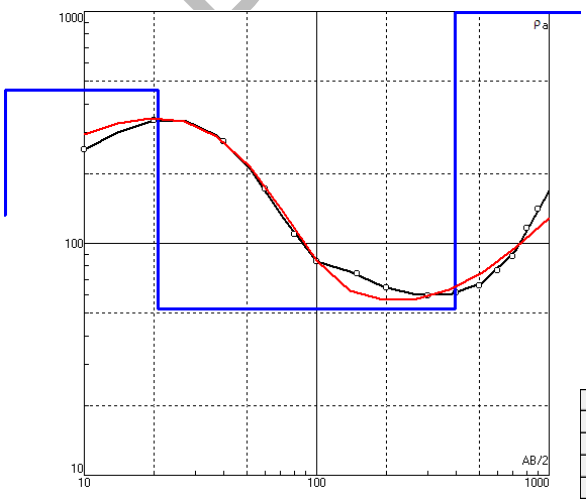

N	1	2	3	4	5						
ρ	133	460	460	52	1615						
h	2.08	7.5	11.2	374							
d	2.08	9.58	20.8	395							
Alt	-2.08	-9.58	-20.78	-394.8							

EE03NE

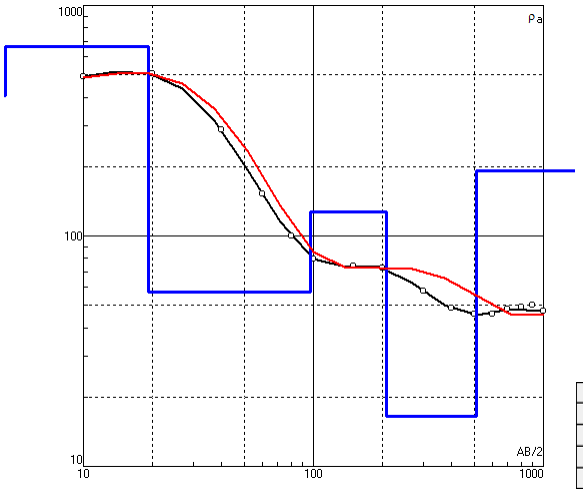

N	1	2	3	4	5	6
ρ	408	661	57.2	127	16.5	191
h	4.31	14.9	77.9	111	301	
d	4.31	19.2	97.1	208	509	
Alt	-4.31	-19.21	-97.11	-208.1	-509.1	

EE01SW

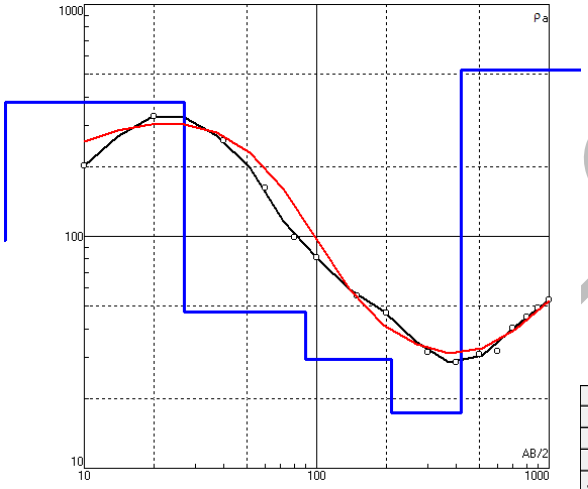

N	1	2	3	4	5	6
ρ	95.9	378	47.3	29.5	17.4	524
h	1.62	25.2	62.8	120	208	
d	1.62	26.8	89.6	210	418	
Alt	-1.62	-26.82	-89.62	-209.6	-417.6	

EE02SW

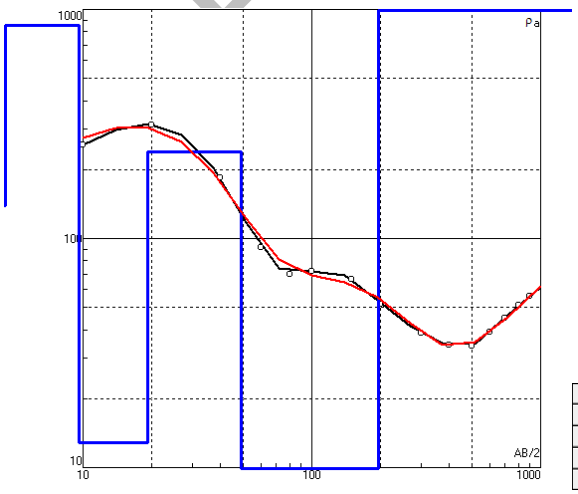

N	1	2	3	4	5	6
ρ	139	853	12.9	239	9.86	3374
h	3.2	6.45	9.52	29.8	147	
d	3.2	9.65	19.2	49	196	
Alt	-3.2	-9.65	-19.17	-48.97	-196	

EE03SW

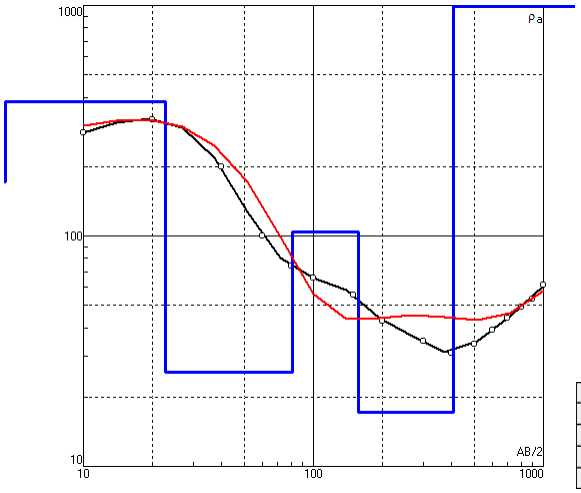

N	1	2	3	4	5	6					
ρ	172	381	25.7	104	17.1	4128					
h	2.01	20.7	58.3	75.9	249						
d	2.01	22.7	81	157	406						
Alt	-2.01	-22.71	-81.01	-156.9	-405.9						

EE04SW

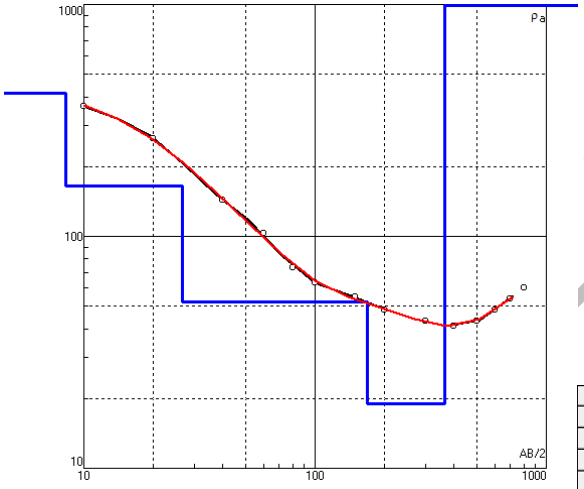

N	1	2	3	4	5						
ρ	413.4	164.2	52.38	18.96	3568						
h	8.348	18.42	142	195.8							
d	8.348	26.77	168.8	364.6							
Alt	-8.348	-26.768	-168.77	-364.57							